SOURCE PARTITIONING OF ANTHROPOGENIC GROUNDWATER NITROGEN IN A MIXED-USE LANDSCAPE, TUTUILA, AMERICAN SAMOA

A THESIS SUBMITTED TO THE GRADUATE DIVISION OF THE UNIVERSITY OF HAWAIʻI AT MĀNOA IN PARTIAL FULFILLMENT OF THE REQUIREMENTS FOR THE DEGREE OF

MASTER OF SCIENCE

IN

GEOLOGY AND GEOPHYSICS

MAY 2016

By
Christopher K. Shuler

Thesis Committee:

Aly I. El-Kadi, Chairperson
Henrietta Dulai
Craig R. Glenn

ACKNOWLEDGMENTS

This work has been greatly improved by the comments and support of Dr. Aly El-Kadi, Dr. Henrietta Dulai, and Dr. Craig Glenn. I must also acknowledge my fellow students Joseph Fackrell, James Bishop, and Christine Waters for showing me the ropes, for sharing their insights and experiences, and for countless discussions about all things scientific or MS-Excel related. I would like to express my sincere appreciation to American Samoa Power Authority (ASPA) and American Samoa EPA (AS-EPA) collaborators: Utu Abe Malae, William Spitzenberg, Katrina Mariner, Danielle Mauga, Tim Bodell, and Mia Comeros, as well as the staff at ASPA, AS-EPA, and the American Samoa Department of Commerce for providing essential data and making countless other contributions, without which this work would not be possible. Finally, I would like to thank Randy DeWees, Hugh Fuimaono, and all of the hard working student interns at American Samoa Community College for their assistance and for weathering rainstorms while sampling wells. This project was made possible through support provided by NOAA's Pacific Regional Integrated Sciences and Assessments Program (PacRISA) and the USGS Water Resources Research Institute Program (WRRIP).

ABSTRACT

On Tutuila, the main island in the territory of American Samoa, nearly all of the island's residents rely on groundwater resources. However, the municipal water system has been subjected to a boil water notice since 2009 due the influence of surface based contamination of groundwater in the island's most developed region, the Tafuna-Leone Plain. The American Samoa EPA has identified three predominant anthropogenic non-point pollution sources of concern: On-Site Disposal Systems (OSDS), agricultural chemicals, and livestock (pig) manure. Development has placed all of these sources within close proximity to many drinking water wells, and water quality analyses indicate that elevated levels of total dissolved groundwater nitrogen (TN) are linked to population density. This suggests the potential to use TN as a tracer of groundwater contamination from the aforementioned activities, which may act as sources of more harmful pollutants. In this study, land-use and hydrological data are integrated with water quality analysis in an N-loading and transport modeling framework for the purpose of quantifying and partitioning the water quality impacts from human land use in the Tafuna-Leone Plain. The integrated framework consists of a numerical groundwater flow model coupled with a GIS based N-loading model and a multi-species contaminant transport model. Nitrogen from each source is modeled as a separate species in order to trace the impact from individual areas. The results are validated with nutrient and isotopic data, and also by assessing historical water quality records and land-use changes over time. Results indicate that OSDS contribute significantly more TN to the aquifer than other sources, and thus should be prioritized in future water quality management efforts.

CONTENTS

Acknowledgments i

Abstract ii

Contents iii

List of tables v

List of figures vi

1. Introduction 1

2. Methods 4

 2.1 - Regional setting and major land-use characteristics 4

 2.2 - Geochemical sample collection and analysis methods 6

 2.3 - Modeling methods 8

  2.3.1 - Modeling framework 8

  2.3.2 - Conceptual Hydrogeologic Model 10

  2.3.3 - MODFLOW Model: Three Dimensional Hydrogeologic Flow Model 11

  2.3.4 - GIS based N-loading model 12

  2.3.5 - MT3DMS Model: Nitrogen fate and transport 15

  2.3.6 - MT3DMS model calibration and attenuation coefficients. 16

3. Results 17

 3.1 - Water quality results 17

 3.2 - Modeling results 19

  3.2.1 - MODFLOW model calibration. 19

  3.2.2 - Sensitivity analysis. 20

  3.2.3 - Attenuation factors and MT3DMS model calibration. 21

  3.2.4 - Assessment of the influence from modeled N-sources. 22

 3.3 – Model validation with isotope mixing model 26

 3.4 – Land-use and management change scenarios. 28

4. Discussion 30

 4.1 – Resource management implications 30

 4.2 - Model validity and limitations 31

 4.3 - Local and regional significance 35

5. Conclusions 36
Appendix A: Observation point selection methods 37
A.1 - MODFLOW observation points. 37
A.2 - MT3DMS observation points. 38
Appendix B: Supplementary information 39
B.1 - Calibration Assessment Measures 39
B.2 - Previously measured rates of N attenuation 40
B.3 – Watershed population density vs. TN concentrations in groundwater 41
B.4 – Details of modifications for land-use and management change scenarios 41
Appendix C: Additional data 45
References 48

LIST OF TABLES

Table 1. Geochemical data from wells, coastal springs, and upland springs……….…..…… pg. 18

Table 2. Modeled %-influence and mass of stored total nitrogen in aquifer……….…...…… pg. 24

Table 3. Results of modeled land-use and management change scenarios……………...…... pg. 29

Table B1. Published and calibrated anthropogenic N attenuation estimates………………... pg. 40

Table C1. Measured water levels from production wells……………………………………… pg. 45

Table C2. Additional geochemical data from water samples …………………….……… pgs. 46 & 47

LIST OF FIGURES

Figure 1. Regional map……………………………………………………….……………..…….pg. 5

Figure 2. Map of sample locations……………………………………...………………..…pg. 7

Figure 3. Schematic of modeling framework……………………………..………...…..…pg. 9

Figure 4. Hydrogeologic conceptual model, map and cross section…………………………..pg. 11

Figure 5. Nitrogen loading model source density grids……………………………….…..…...pg. 14

Figure 6. MODFLOW groundwater head and calibration results…..…………………...……pg. 19

Figure 7. Results of sensitivity tests………………………………………………………….....pg. 20

Figure 8. MT3DMS model calibration results……………………………...………….pg. 21

Figure 9. Modeled groundwater TN concentration distribution maps…………………..……pg. 23

Figure 10. Modeled TN concentrations and source fractions at observation points…......….pg. 24

Figure 11. Assessment of calibration uncertainty with Monte Carlo technique…………….. pg. 25

Figure 12. Nitrogen isotope mixing model results……………………………………….…...pg. 27

Figure 13. Comparison of trends in historical pig census and water quality data…………...pg. 33

Figure 14. Assessment of model steady state conditions…………………………….……....pg. 33

Figure A1. Example geometry for hypothetical observation points………………………...…pg. 37

Figure B1. Comparison between groundwater TN and population density……………....…pg. 41

Figure B2. Leone-Wastewater-Collection Zone scenario……………………………….…….pg. 41

Figure B3. Removal of existing wastewater collection system scenario…………………...….pg. 42

1. INTRODUCTION

On many small tropical volcanic islands, groundwater resources are critically important, yet they can also be vulnerable to anthropogenic non-point source contamination. Groundwater provides about 90% of the drinking water on Tutuila, the main island in the territory of American Samoa (AS-DOC, 2013). However, much of the island's municipal water is unsafe to drink without disinfection, and has been under a boil-water-advisory since 2009 (Chen, 2013). Groundwater in Tutuila's most populated area, the Tafuna-Leone Plain, is especially vulnerable due to the region's geologic setting and high development density. The plain's young lava flows and thin ash units are characterized by an exceptionally high infiltration capacity (Eyre, 1994). This, combined with the high annual rainfall, creates highly productive aquifers. However, such conditions also limit the soil's ability to attenuate contaminants, leaving the groundwater susceptible to rapid transport of pollutants derived from surface activities (Kennedy/Jenks/Chilton, 1987). Previous investigations have linked turbidity and *E.coli* detections in wells to heavy rain events, further supporting the link between subsurface transport pathways and contamination from surface based pollutants (ASPA, 2012). The American Samoa Environmental Protection Agency (AS-EPA) recognizes a high groundwater contamination potential from non-point sources, including: septic tanks and cesspools, also known as On-Site wastewater Disposal Systems (OSDS), agricultural applications of fertilizers and pesticides, and manure from small backyard scale pig rearing operations termed piggeries (AS-EPA, 2010). These sources of groundwater pollution pose both human health and environmental water quality risks. Wastewater and animal manures contain pathogens such as bacteria, protozoa, and viruses (Burkholder et al., 2007; Whittier & El-Kadi, 2009). In addition, inefficient agricultural practices can leach nutrients and toxic organic compounds into aquifers (Oki & Giambelluca, 1987). Wastewater influence on drinking water supplies has been identified as a major cause of waterborne disease outbreak, even in developed countries (Hrudey & Hrudey, 2007), and nutrient pollution from these sources has been linked to degradation of environmental water quality on other tropical islands (Dailer et al., 2012; Bishop et al., 2015).

On Tutuila, the primary anthropogenic groundwater pollutants of concern are: pathogens, excessive nutrients, pesticides, and herbicides (Eyre, 1994; Kantor et al., 1996).

Unfortunately, directly testing for many of these constituents is limited by low contaminant concentrations, non-conservative behavior, and high analysis costs. However, in other settings elevated levels of groundwater nitrogen have been clearly linked to wastewater, manure, and agricultural contamination (El-Kadi & Yabusaki, 1996; Gardner & Vogel, 2005; Verstraeten et al., 2005; Burkholder et al., 2007). A study by Mair & El-Kadi (2013) found that on Oahu, Hawaii, concentrations of groundwater nitrate (NO_3^-) could be used as a predictive indicator for the occurrence of other harder to measure anthropogenic contaminants such as solvents, fumigants, and pesticides. Nitrate concentrations in Tutuila's aquifers are generally below the EPA drinking water quality regulatory limit of 710 $\mu M_{(N)}$ (10 mg/L), and are thus not a health risk themselves. However, both groundwater and surface water dissolved nitrogen concentrations on the island are correlated with population density in watersheds (DiDonato, 2005; Appendix B, Fig. B1). This suggests that total dissolved groundwater nitrogen (TN) is a suitable tracer of human land-use impact on groundwater quality.

Integrating geochemical tracers with numerical contaminant-transport models is a widely used practice for tracking groundwater contaminants, although relatively few studies have applied this combined approach in volcanic island settings. The isotopic signature of nitrogen in groundwater nitrate ($\delta^{15}N$) is a common tracer for distinguishing between different N-sources (Kendall & Aravena, 2000; Hunt, 2007), and isotope mass balance has been used to partition relative contributions from each source (Cole et al., 2006). Additionally, GIS based N-loading models are frequently used to account for the spatial distribution of nitrogen sources, especially when sources are co-linearly distributed throughout the landscape, such as they are on Tutuila (Valiela et al., 1997; Whittier & El-Kadi, 2009). More comprehensive studies have coupled N-loading models with numerical groundwater flow and contaminant transport models, such as MT3DMS (Zheng & Wang, 1999), to simulate nitrogen transport from point and non-point sources (Conan et al., 2003; Almasri & Kaluarachchi, 2007; Morgan et al., 2007). This study applies similar methods in a small tropical island setting, to answer a persistent question about which management actions are needed to reduce drinking water contamination potential.

The specific objectives of this research are:

1) Quantification of groundwater quality impact from – OSDS, agriculture, and piggeries – on the Tafuna-Leone Plain.
2) Development of a predictive tool for assessing the potential risk of groundwater contamination at future well development locations in the Tafuna-Leone Plain.
3) Evaluation of groundwater quality impacts due to future land-use change or management efforts on Tutuila.
4) Development of a geochemical sampling and modeling framework that is adaptable for contamination risk assessment on similar tropical islands.

To achieve these objectives, the distribution of groundwater TN is used to trace and rank the relative water quality impact of the island's three primary contamination sources - OSDS, agriculture, and piggeries. Nutrient and stable isotope data from wells and springs are integrated in a groundwater loading and transport modeling framework to simulate TN concentrations and N-isotopic values in the Tafuna-Leone Plain. The modeling framework is intended to be used as a resource management tool, which can be modified to explore the potential effects of proposed management actions. The model is used to test a number of land-use management scenarios that were collaboratively developed with water resource management stakeholders on Tutuila. The results of this study are useful for prioritizing water resources management efforts, guiding future water development, and providing a conceptual framework for understanding and quantifying groundwater contaminant transport on Tutuila.

2. METHODS

2.1 - REGIONAL SETTING AND MAJOR LAND-USE CHARACTERISTICS

The Samoan Archipelago is located in the tropical South Pacific Ocean, about halfway between New Zealand and the Hawaiian Islands. The island of Tutuila serves as the political and cultural center of the Territory of American Samoa, and at 137 km^2, is the largest island in the territory (Fig. 1). The climate is hot and humid, with plentiful rainfall averaging 3,000 to 6,000 mm/year (Craig, 2002). Tutuila can be divided into two primary geographic regions: a fairly pristine mountainous interior and a flat coastal (Tafuna-Leone) plain, where the majority of the island's population resides. The island's inhabitants are distributed among 74 distinct villages that have historically controlled the necessary residential and agricultural infrastructure to be self-supporting administrative units (Coulter, 1941; Perry, 1986). As a result, Tutuila's landscape is well mixed and poorly zoned, with each village containing a fairly even distribution of the land-use activities that act as non-point groundwater pollution sources.

Primary land-use types examined in this study are 1) piggeries, 2) agricultural plantations, and 3) residential areas (with OSDS units). Raising pigs is common for many of the island's families, and remains a staple of traditional culture. Despite the cultural importance of pigs, awareness of their potential to pollute environmental waters has recently grown (NRCS, 2007). Pig waste is high in nutrients, creates a large biological oxygen demand, and is a source of pathogens and parasites (AS-IPMC, 2004; Burkholder, 2007). Agriculture in American Samoa is widespread, and more than half of all arable land is under cultivation. A significant portion of the island's food supply is grown locally, and the island's 5,800 farms produce about $50 million worth of products annually (US-DOA, 2011). A number of the island's farms are thought to be heavy users of synthetic fertilizers, herbicides, and pesticides, many of which are illegally imported and subjected to poor regulation (Miller, 2013). About 60% of Tutuila's residents rely on OSDS units consisting of cesspools or often improperly constructed septic systems for wastewater disposal (DiDonato & Paselio, 2006). The remaining 40% are served by municipal wastewater collection systems. Prevalent OSDS have been widely implicated as sources of groundwater contamination on Tutuila, and much of the island's thin soil is poorly developed with limited contaminant attenuation capacity (Falkland, 2002). Despite this fact, a large percentage of the island's OSDS units are cesspools, where raw untreated wastewater is allowed to infiltrate directly into the ground.

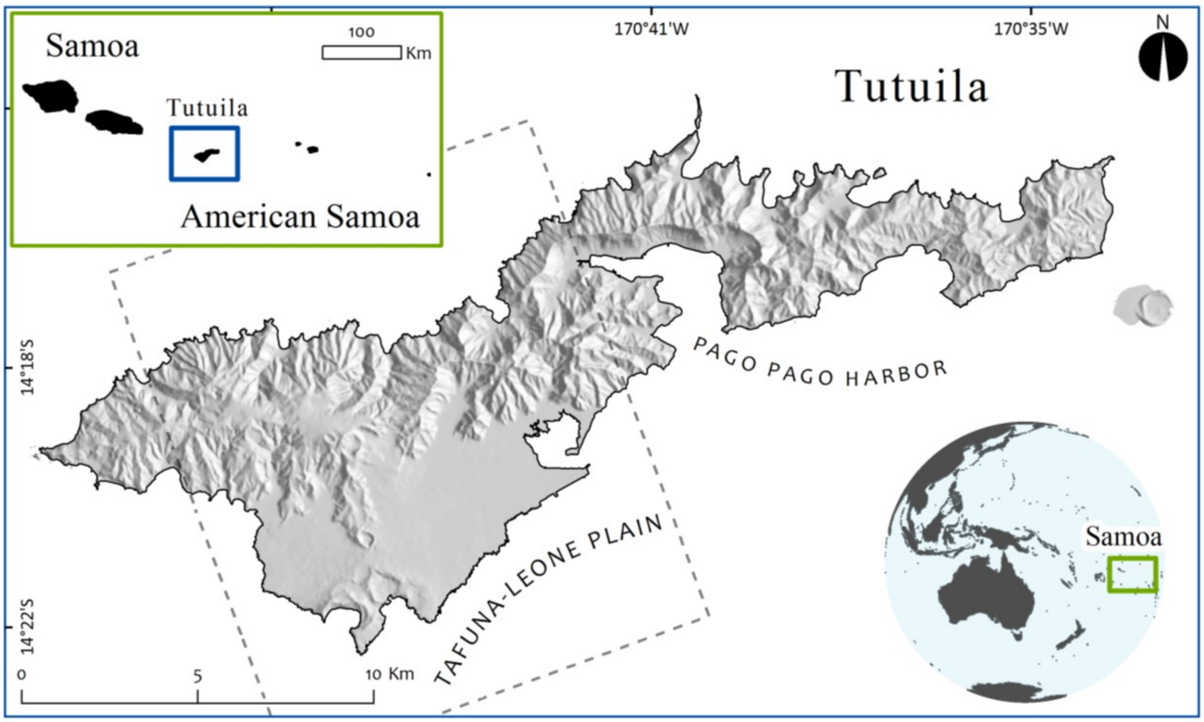

Fig. 1. Location of the study area. ***Dashed line*** **indicates the numerical model no-flow boundary.**

2.2 - GEOCHEMICAL SAMPLE COLLECTION AND ANALYSIS METHODS

Measurements of groundwater TN and $\delta^{15}N$ were incorporated in the MT3DMS model as observation points and served as calibration and validation data. To obtain these data, groundwater sampling was conducted at 32 wells and springs in the Tafuna-Leone Plain region between August 2013 and August 2015 (Fig. 2). Most samples were collected during Samoa's dry season (June to August), although 10 repeated samples were collected at four sites during both seasons to ensure that temporal variation during the sampling period was insignificant. For locations that were sampled multiple times (n = 1 to 10), the mean value from all samples taken at the site was used in model calibration. Production wells were sampled at wellhead collection ports, and pumps were run long enough to ensure effective purging of the well bore. Coastal springs were sampled with a peristaltic pump and a handheld piezometer, which was temporarily installed in each spring. All samples were filtered on-site with 0.45 µm hydrophilic polyethersulfone capsule filters that were purged long enough to ensure adequate flushing of the water delivery line and to avoid carry-over contamination between samples. Temperature, salinity, pH, dissolved oxygen, and turbidity were measured in situ with a YSI multiparameter sonde. All samples were collected in triple-rinsed, acid washed 60 ml HDPE bottles and were cooled during transport to storage facilities. Nutrient samples were refrigerated for short-term storage (< 2 weeks) or frozen when longer storage times were necessary. Nitrogen isotope samples were frozen the day of collection and thawed immediately prior to analysis. Nutrient samples were analyzed within 1 month, while $\delta^{15}N$ samples were analyzed within 4 months of collection.

Nutrient samples were analyzed for concentrations of dissolved phosphate (PO_4^{3-}), silicate (SiO_4^{4-}), nitrate (NO_3^-), nitrite (NO_2^-), ammonium (NH_4^+), total nitrogen (TN), total organic carbon (TOC), and total phosphorus (TP) by the University of Hawaii SOEST Laboratory for Analytical Biogeochemistry, using the methods described in Grasshoff et al. (1983) and Armstrong et al. (1967) (Results tabulated in Appendix C, Table C2). Analytical error was assessed by comparing duplicate samples that comprised over 10% of the sample set. Since coastal spring samples are composed of both oceanic and fresh water, nutrient concentrations in these samples were normalized to the assumed freshwater salinity (0.1) of their groundwater end-member. This was done with an un-mixing calculation (Hunt and Rosa, 2009) based on a measured oceanic end member from Tutuila. This calculation allowed direct comparison between fresh well samples and salty coastal spring samples.

Nitrogen isotope values were measured at the University of Hawaii's Stable Isotope Biogeochemistry Lab using the denitrifier method of Sigman et al. (2001). All samples were analyzed on a Thermo Finnigan MAT 252 Mass Spectrometer using a continuous flow GC-interface. Isotopic results are expressed in per mil (‰) notation relative to AIR (the primary stable isotope standard for N). Data were corrected with the internationally recognized NO_3^- isotope standards USGS 32, USGS 34, and USGS 35. Over 5% of the sample set consisted of duplicate samples, which were used to assess analytical error.

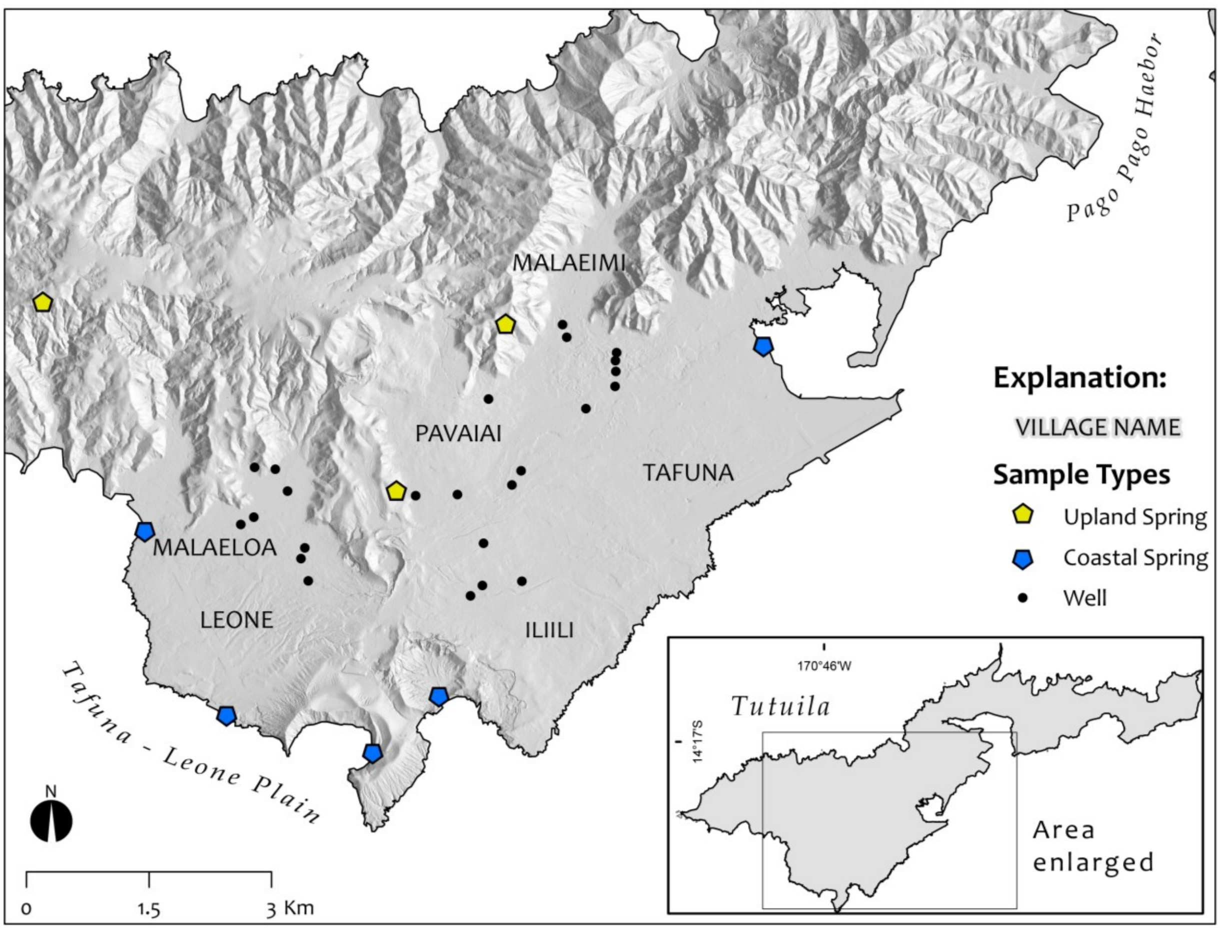

Fig. 2. Locations of groundwater quality sampling sites.

2.3 - MODELING METHODS

2.3.1 - Modeling framework

To simulate the fate and transport of groundwater TN, this study combined geochemical observations with an integrated set of models to simulate groundwater flow, N-loading, and contaminant transport (Fig. 3). The groundwater flow field was estimated with the widely used numerical model MODFLOW (Harbaugh, 2005), and N-loading was estimated with a GIS based model that incorporated land-use data and estimates of non-point source TN loading rates. The outputs of these models were combined in an MT3DMS multi-species contaminant transport model to simulate TN movement through the aquifer. The models were pre-and post-processed with the Groundwater Modeling System, a commercially available software package (http://www.aquaveo.com). Models were calibrated with measured water levels and values of groundwater TN from water quality samples. The modeling framework quantified the amount of TN originating from each non-point source, effectively tagging each sources' fractional N-contribution to the groundwater.

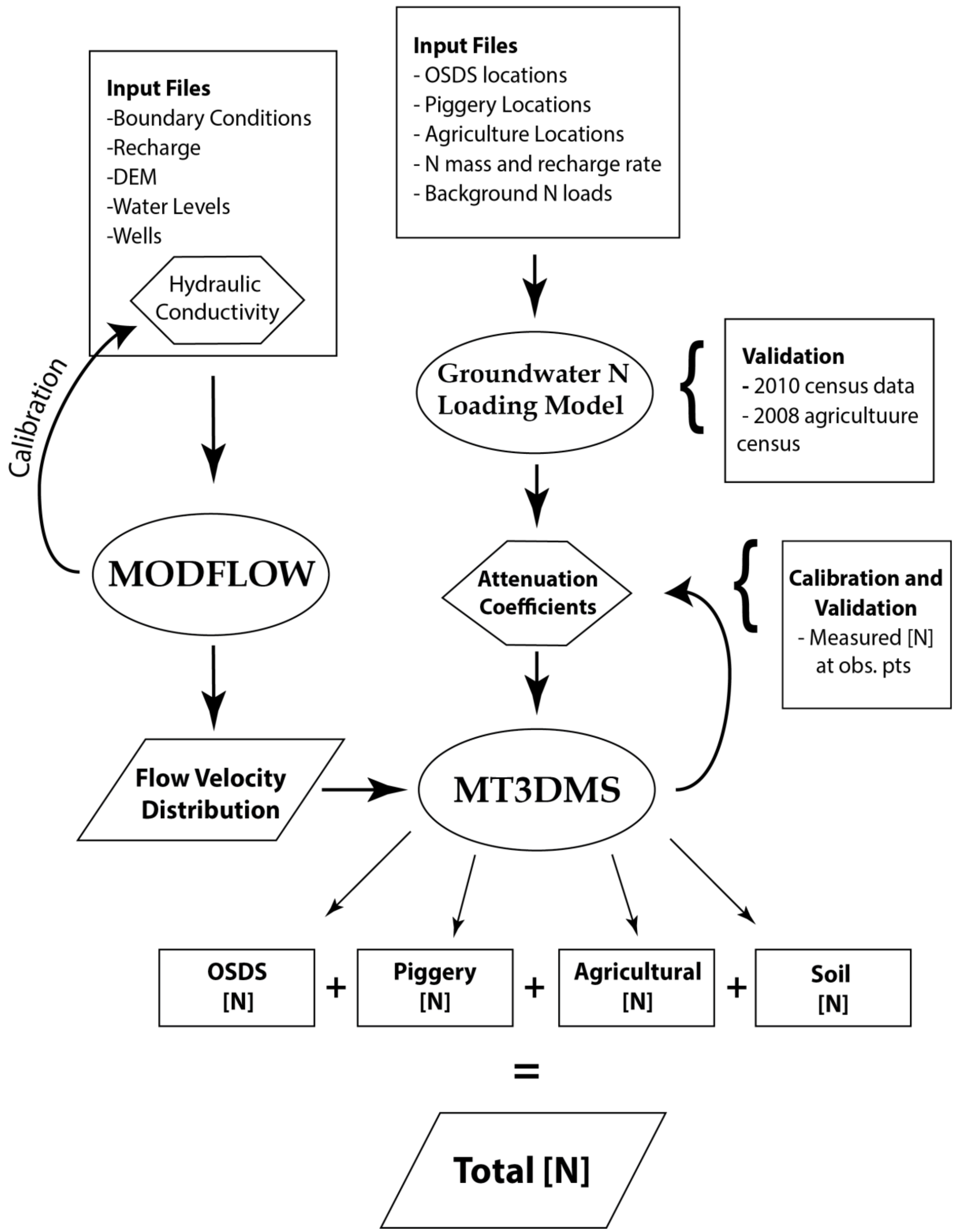

Fig. 3. Schematic of the modeling framework used in this study. Anthropogenic impact to groundwater, represented by Total Nitrogen, is evaluated by quantifying N-loading, attenuation, and transport from the four modeled non-point N-sources.

2.3.2 - Conceptual Hydrogeologic Model

The island of Tutuila is composed of four overlapping basaltic shield volcanoes formed by hot spot processes roughly 1.5 to 1.0 Ma (McDougall, 1985). During the Holocene, a rejuvenation stage eruptive event accreted the Tafuna-Leone Plain upon the eroded southwestern flank of the older shield unit. The Tafuna (eastern) side of this plain is primarily composed of highly permeable thin-bedded pahoehoe and a'a flows. The Leone (western) side contains interbedded lava flows and ash layers from material that was blown westward by the prevailing southeast trade winds during eruptions (Stearns, 1944). These ash beds reduce the vertical hydraulic conductivity of the Leone unit (Izuka et al., 2007). A north-south trending rift zone runs down the middle of the plain and is marked by pyroclastic deposits and cinder/ash cones (Fig. 4a). The older-volcanic shield to the north and underlying the plain (the Taputapu shield) has been characterized as a low-permeability formation, although it is undoubtedly structurally heterogeneous with alternating zones of higher and lower hydraulic conductivities (Knight Enterprises, 2014). This unit likely contains physical features such as dikes, faults, or perching layers that make the overall permeability relatively low (Walker & Eyre, 1995). A carbonate wedge also sits between the younger Tafuna-Leone Plain and the underlying older-volcanic unit (Fig. 4b). This thin wedge of unknown permeability was presumably deposited in a lagoon environment behind a now drowned barrier reef as the island experienced an episode(s) of subsidence (Stearns, 1944). The Tafuna-Leone Plain was erupted through and onto the carbonate platform, and the contact between the two sits at a depth of roughly 50-90 m below sea level. The younger volcanic rocks of the plain hold the island's most productive, yet vulnerable aquifers.

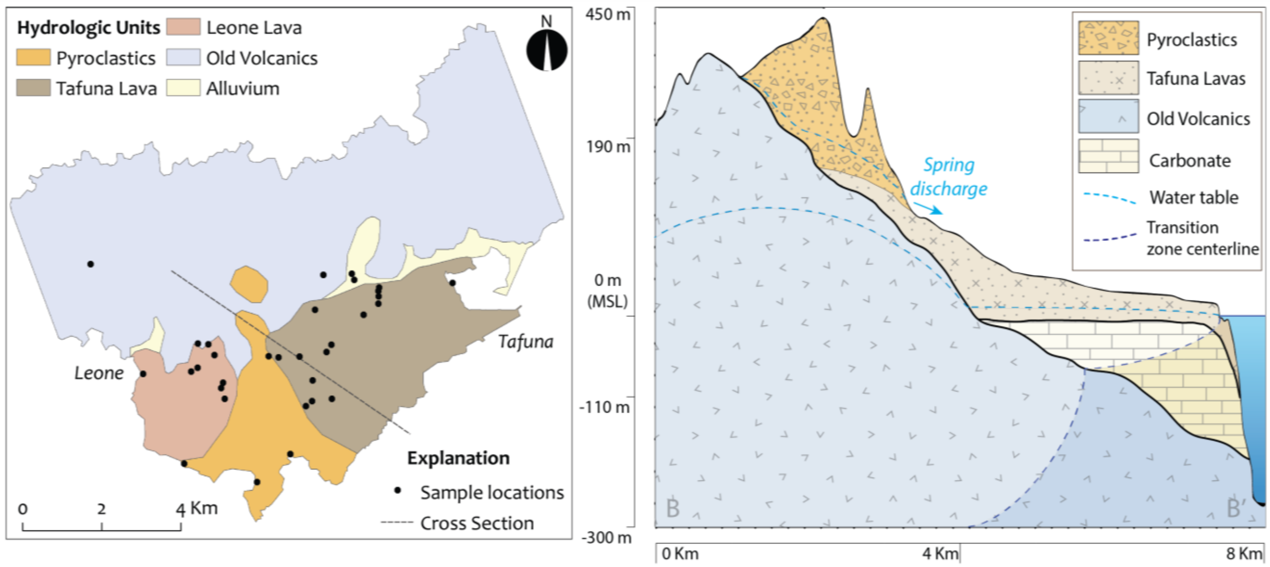

Fig. 4a (left). The model's areal extent and hydrogeologic units. 4b (right). Conceptualized cross section through the Tafuna-Leone Plain, Olotele Mountain and the older-volcanic unit. *Darker shading* indicates estimated areas of saltwater saturated rock. Subsurface features in 4b are not necessarily to scale.

2.3.3 - MODFLOW Model: Three Dimensional Hydrogeologic Flow Model

Groundwater flow was simulated with the steady state finite-difference groundwater model, MODFLOW-2005 (Harbaugh, 2005). The flow model developed for this study employed the conceptual foundation of a pre-existing MODFLOW model created by Izuka et al. (2007). Most of the parameters and data used in the Izuka et al. model were adopted including: cell size, number of layers, boundary locations and conditions, hydrologic unit locations, stream conductance, production well locations, pumping rates, and recharge rates. The Izuka et al. model was 10 layers deep with a cell size of 91 x 91 m. It was originally calibrated with water levels taken at 6 monitoring wells and streamflow measurements from 11 USGS gauging sites. However, new hydrologic monitoring data for Tutuila were gathered for this study, so updated head levels in wells were substituted as observation points, and the model was re-calibrated to reflect current conditions. Groundwater recharge from the Izuka et al. model was estimated with the soil water budget method (Thornthwaite & Mather, 1955) and included mountain-front-recharge zones in the northern Tafuna-Leone Plain to simulate surface water infiltration where streams encountered more permeable rocks in the plain.

The MODFLOW model re-calibration was based on 17 new measured values of groundwater head from shutdown production wells, which resulted in slightly different values of hydraulic conductivity (*K*). Details regarding observation point selection are given in Appendix A. Climate data from the Pago Pago airport and well data from American Samoa Power Authority (ASPA) files show that pumping rates and climactic conditions have been relatively consistent since 2007, indicating that the Izuka et al. (2007) model parameters should still be representative of current conditions. Model performance (comparison of modeled vs. observed values) was assessed with correlation and error-based metrics of model fit including: 1) the coefficient of determination (r^2), 2) the least mean squares regression coefficients (*slope and intercept*), 3) the modified index of agreement (d_1), 4) the mean average error (*MAE*), and 5) the mean relative error (*MRE*). These metrics are discussed in Appendix B, section B.1.

2.3.4 - GIS based N-loading model

To simulate land-use N-inputs, a grid-based N-recharge model was developed. The model domain was divided into 10,438 cells, each measuring 91 m x 91 m. The number of individual pigs and OSDS units, and the fraction of agricultural land in each cell were used to assign a separate density for each N-source to every cell (Fig. 5). Nitrogen from natural soil sources was accounted for by equally distributing about 6 µM of TN to the recharge in all cells, which made modeled background levels match measured values at pristine sample sites. Each cell was assigned four constant N-recharge rates for each of the four sources, and these rates were dependent on the calculated densities of each source in the cell. Considering each of the four N types separately allowed them to be input into the MT3DMS model as four distinct species of TN (OSDS-N, pig-N, agricultural-N, and soil-N). Since the four N-types represented a fractional component of the TN load, their modeled concentrations could be summed to compare to measured TN values.

Locations and sizes of piggeries were obtained from the annually updated AS-EPA Piggery Compliance Program GIS dataset (Zennaro, 2007; AS-EPA, 2015). Data from the year 2014 were used to determine pig densities for each model cell. The N-loading rate from pig waste was based on an estimated release rate of 14 kg of TN per pig, per year (AS-EPA, 2013). An additional 0.038 m^3 of water per pig was added to the model's recharge to account for estimated water use in Samoan piggeries (AS-IPMC, 2004).

Agricultural land use was obtained from a vegetation mapping survey that was based on remote sensing methods and field surveys (Liu et al., 2011). Although fertilizer application rates could not be found for American Samoa, it was assumed that application rates are similar in the independent nation of Samoa where cultural practices and socioeconomic standards are analogous to those in American Samoa. The World Bank (2015) reports an average synthetic fertilizer application rate of 2.81 kg of N per ha of arable land, per year in Samoa. Due to data limitations regarding the types and rates of agricultural applications, in this study, it was assumed that synthetic fertilizer applications are evenly distributed temporally and spatially between all areas that are classified under agricultural land use.

Locations of OSDS units were indirectly determined, since no direct survey data were available. This was accomplished by taking the locations of buildings and geospatially subtracting those assumed to be connected to a sewer line. A geographic shapefile of buildings was obtained from the American Samoa Department of Commerce, and structures with a footprint of $< 120\ m^2$ in size were removed from the coverage to exclude sheds or other small buildings that were unlikely to contain a bathroom. The remaining buildings were assumed to be households or businesses with a toilet, and their estimated number of 5,734 was validated with U.S. Census data that reported the number of households in the region to be 5,682 (AS-DOC, 2013). As-built drawings of the sewer main lines and connections from ASPA were used to develop a 10 m sewer line buffer zone. Households that were located in this zone were assumed to have municipal wastewater collection service and were removed, leaving the remaining households as ones that must use some type of OSDS. The ratio of OSDS to sewered households (3,200:2,530) was also validated with census data (2,800:2,880). The above discrepancy was accepted because it was suspected that the number of households on sewers was over reported in the census data; where statistics from a number of villages lacking sewer main lines contained households that enigmatically reported a sewer connection. The amount of nitrogen loaded to groundwater per OSDS unit was calculated based on a direct measurement of TN in Tutuila wastewater taken from the Utulei Wastewater Treatment Plant. Samples of raw and settled effluent from the plant had an average TN concentration of 1116.1 μM (15.6 mg/L). This value was multiplied by an estimated $0.26\ m^3$ of wastewater discharged per person per day (WSDH, 2002), which was then multiplied by the average Tutuila household size of 5.6 people to derive the loading rate of just over 8 kg of TN per OSDS unit, per year.

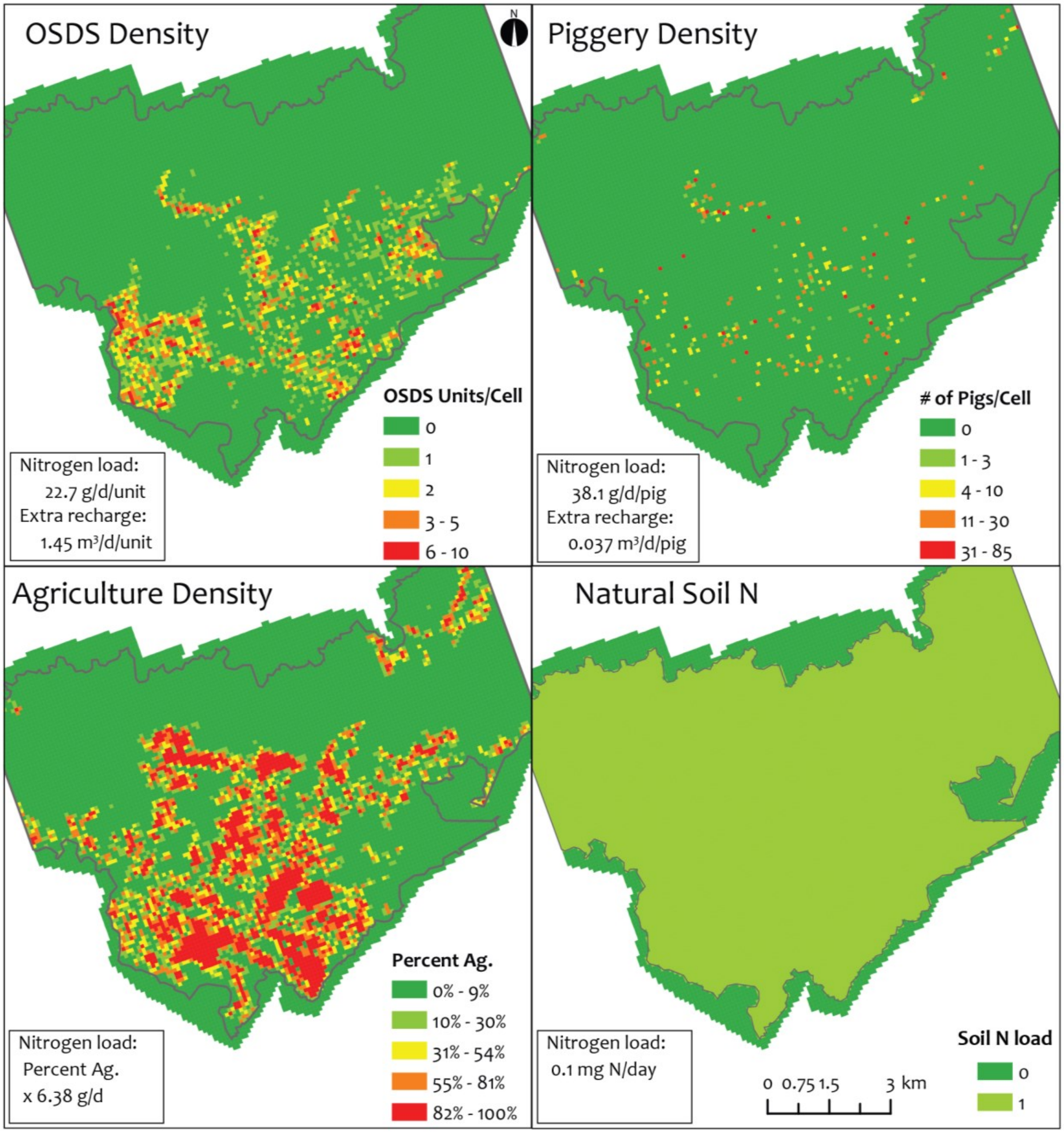

Fig. 5. N-source density grids used as input to the N-loading model.

2.3.5 - MT3DMS Model: Nitrogen fate and transport

To simulate N-transport, MT3DMS was used to integrate the MODFLOW flow field with the GIS N-loading model. Measured TN values from water samples were incorporated into the MT3DMS model as observation points. Details regarding the assignment of observation point values are given in Appendix A. The modular multi-species transport model MT3DMS accounts for contaminant advection and dispersion in groundwater. The model combines three transport solution techniques including the standard finite difference method, the particle-tracking-based Eulerian-Lagrangian methods, and the higher-order finite-volume total-variation-diminishing method. These methods are used simultaneously to balance the limitations that each has in modeling the combined processes of advection and dispersion (Zheng & Wang, 1999).

The MT3DMS model simulates dispersion effects with a single longitudinal dispersivity coefficient ($\boldsymbol{a_L}$) and uses fixed ratios of this coefficient to simulate dispersivity on the transverse and vertical axes. Reported estimates of $\boldsymbol{a_L}$ in basalt aquifers range from 0.6 m to 1370 m, however, this factor is primarily controlled by the spatial-scale of groundwater flow paths (Gelhar et al., 1992; Schulze-Makuch, 2005). Xu and Eckstein (1995) suggest the following relationship to estimate $\boldsymbol{a_L}$ based on the scale of flow:

$$\alpha_L = 0.83 \times [\log(L)]^{2.414} \tag{1}$$

Where $\boldsymbol{L}$ is the length of the groundwater flow path from source to sink (in meters). The flow domain for the Tafuna-Leone Plain ranges from about 2-8 km, which results in values of $\boldsymbol{a_L}$ that range between 10 and 24 m. A value of 15 m was chosen as the model input parameter, and sensitivity tests revealed minimal variations in model output through this range. This value is fairly consistent with measured and modeled values of $\boldsymbol{a_L}$ in the Hawaiian Islands where estimates range from 25 to 75 m (Izuka, 2011; Glenn et al., 2013). In this study, the ratios of transverse to longitudinal dispersivity and vertical to longitudinal dispersivity were chosen to be 0.2 and 0.1 respectively (Gelhar et al., 1992).

2.3.6 - MT3DMS model calibration and attenuation coefficients.

The transformation and attenuation of nitrogen between its source and the groundwater is an important yet complex subsurface process that controls the final groundwater composition at wells. Volatilization, adsorption, denitrification, and biological uptake may all act to change the speciation and TN concentration of recharging waters as they travel to the water table. Many studies have quantitatively assessed these processes (Valiela et al., 1997; Ling & El-Kadi, 1998; Almasri & Kaluarachchi, 2007). However, since the factors that control N-attenuation on Tutuila are poorly constrained, a simplified approach was used in this study to represent, but not explicitly model, all attenuation processes. Each of the three anthropogenic N-types (Pig-N, OSDS-N, and Ag.-N) was multiplied by a separate attenuation coefficient to account for all attenuation processes. Conservative nitrogen transformations (changes in speciation) were ignored since the model only considered total nitrogen. Preliminary sensitivity tests indicated that model results were most sensitive to changes in these attenuation coefficients, so these coefficients were parameterized with model calibration. Although in reality, the coefficients represent independent processes, in the model, they had the ability to offset each other. When calculating the modeled TN value, a decrease in one coefficient could make up for an increase in another, which created many non-unique model solutions. To work around this complication, a Monte Carlo calibration technique was used to repeatedly run the model with unique sets of the three coefficients. The MT3DMS model was run over 5200 times with randomly generated sets of attenuation coefficients that each ranged between 0% and 100% attenuation. The aforementioned metrics of model fit were calculated for each run, and the set that optimized the fit between the model and the data was selected.

3. RESULTS

3.1 - WATER QUALITY RESULTS

Nutrient analysis of water samples generally showed higher TN concentrations at sites located in more developed areas. As should be expected, upland springs typically had lower concentrations than production wells or coastal groundwater samples. Coastal spring TN concentrations were most variable, reflecting different proportions of up-gradient development. Wells in developed areas had average TN concentrations ranging from 70 to 100 µM, whereas well fields farther from development had lower levels of TN. For example TN concentrations in the semi-urbanized Leone well field were three times higher than those observed in the Malaeloa well field, which lies up gradient from any villages. Most of the TN in well samples was in the form of NO_3^- with little to no NO_2^- or NH_4^+. The proportion of NO_3^- in the TN from all well samples ranged between 83% and 98%, with an average of 89.7 ± 4.4%. Analytical uncertainty for all analyses was assessed with the standard error of the estimate between blind duplicate samples. This yielded an uncertainty of ± 1.2 µM, ± 3.2 µM, and ± 0.33‰ for NO_3^-, TN, and $\delta^{15}N$ analyses, respectively (Table 1).

Dissolved oxygen values were recorded during sample collection to help characterize the aquifer condition (Table 1). Most samples in the study area were well oxygenated, having dissolved oxygen concentrations between 4.5 and 7.4 mg/L in wells, and between 2.9 and 7.4 mg/L in coastal springs. Upland springs and streams that recharge the aquifer in pristine high elevation settings, showed $\delta^{15}N$ values of 3‰ to 5‰, which is consistent with an atmospheric or soil nitrogen source. Most coastal spring samples in developed areas showed high overall TN concentrations and $\delta^{15}N$ values exceeding 9‰. Assuming N acts conservatively in the groundwater, this suggests an enhancement in N-loads from wastewater or manure sources. Well waters showed intermediate $\delta^{15}N$ values, 5-9‰, which also increased with the degree of development in each well's recharge area.

Table 1. Geochemical data from well, coastal spring (C. spring), and upland spring (Up. spring) samples used as observation points in the MT3DMS model

Name	Type	n	Latitude	Longitude	DO [(a.)] (mg/L)	NO_3^- [(b.)] (μM)	TN [(c.)] (μM)	$\delta^{15}N_{(NO3-)}$ [(d.)] (‰)
Iliili-62	Well	1	-14.34761	-170.74863	5.6	65.4	70.2	8.1
Iliili-76	Well	1	-14.34646	-170.74725	6.9	57.2	58.2	7.7
Iliili-84	Well	10	-14.34597	-170.74276	5.3 ± 0.8	69.1 ± 13.9	78.3 ± 6.5	6.2 ± 0.2
Iliili-167	Well	1	-14.34178	-170.74714	7.0	119.7	126.3	7.5
Leone-70	Well	1	-14.33971	-170.77473	6.5	117.9	117.1	9.1
Leone-80	Well	1	-14.33889	-170.77324	7.4	88.4	87.6	5.8
Leone-83	Well	1	-14.33600	-170.76941	7.3	58.2	66.4	4.9
Leone-91	Well	1	-14.34232	-170.76744	6.4	122.0	127.4	10.7
Leone-93	Well	10	-14.34348	-170.76787	6.6 ± 0.9	68.5 ± 7.6	83.4 ± 17.7	9.2 ± 0.6
Leone-119	Well	2	-14.34596	-170.76707	5.5 ± 0.1	74.6 ± 8.1	81.5 ± 5.0	9.1 ± 2.2
Malaeimi-67	Well	1	-14.31895	-170.73769	5.2	54.7	64.4	7.4
Malaeimi-85	Well	1	-14.32580	-170.74657	7.3	52.9	61.6	8.5
Malaeimi-89	Well	10	-14.31754	-170.73821	5.8 ± 0.9	40.1 ± 6.8	47.2 ± 3.4	6.0 ± 0.3
Malaeloa-168	Well	1	-14.33358	-170.77082	7.0	23.8	31.5	6.0
Malaeloa-169	Well	2	-14.33337	-170.77319	7.2 ± 0.1	28.1 ± 1.1	29.3 ± 1.4	5.9 ± 0.3
Pavaii-171	Well	3	-14.33373	-170.74288	7.3 ± 0.1	84.2 ± 6	83.8 ± 3.3	9.0 ± 0.4
Pavaii-172	Well	1	-14.33531	-170.74393	6.9	79.7	81.3	8.5
Pavaii-177	Well	1	-14.33637	-170.75013	7.1	69.0	79.4	8.4
Pavaii-178	Well	1	-14.3365	-170.75485	7.4	33.7	39.2	7.7
Tafuna-33	Well	10	-14.32436	-170.73219	6.0 ± 1.0	72 ± 13.3	80.2 ± 12.3	7.6 ± 0.3
Tafuna-61	Well	1	-14.32686	-170.73554	5.7	81.5	99.9	7.2
Tafuna-72	Well	1	-14.32154	-170.73219	6.1	62.3	70.2	7.5
Tafuna-77	Well	1	-14.32273	-170.73214	4.5	47.0	53.5	7.1
Tafuna-81	Well	1	-14.32065	-170.73203	5.2	46.2	46.2	6.9
CSp-1	C. spring	2	-14.31969	-170.71535	4.5 ± 0.4	42.2 ± 6.2	81.7 ± 6.9	9.1 ± 0.2
CSp-2	C. spring	2	-14.34026	-170.78564	7.0 ± 1.9	94.5 ± 5.9	92.6 ± 9.0	10.0 ± 1.2
CSp-3	C. spring	1	-14.36480	-170.75971	2.9	1.7	4.3	6.7
CSp-4	C. spring	1	-14.36067	-170.77632	5.0	4.7	21.6	4.4
CSp-5	C. spring	1	-14.35852	-170.75219	6.6	49.1	53.0	2.8
USp-1	Up. spring	1	-14.31782	-170.74469	7.4	3.1	4.3	3.4
USp-2	Up. spring	1	-14.33632	-170.75709	7.3	9.8	15.7	3.3
USp-3	Up. spring	1	-14.31546	-170.79753	6.7	0.0	1.2	--

**Uncertainties shown with ± symbol indicate the standard deviation from averaged repeat sample values. Uncertainties for data without a symbol are given below.*

***a.** YSI factory reported instrument uncertainty ± 0.1 mg/L for DO*

***b.** Nitrate uncertainty: ± 1.2 μM*

***c.** Total N uncertainty: ± 3.2 μM*

***d.** $\delta^{15}N$ uncertainty: ± 0.33‰*

3.2 - Modeling results

3.2.1 - MODFLOW model calibration.

As noted above, the MODFLOW model used in this study incorporated input parameters taken directly from the Izuka et al. (2007) model with the exception of ***K*** values, which were re-calibrated based on updated water level measurements. Figure (6a) shows the locations of the 17 new calibration points and the MODFLOW calculated potentiometric surface. Good calibration was achieved, with a *MAE* of 0.14 m (maximum of 0.37 m and minimum of 0.002 m). The (r^2) was 0.97 and the slope and intercept were 0.94 and 0.11, respectively (Fig. 6b). Unfortunately, no water level data were available for a large portion of the older-volcanic unit, which may contribute to uncertainties in modeling results for this region.

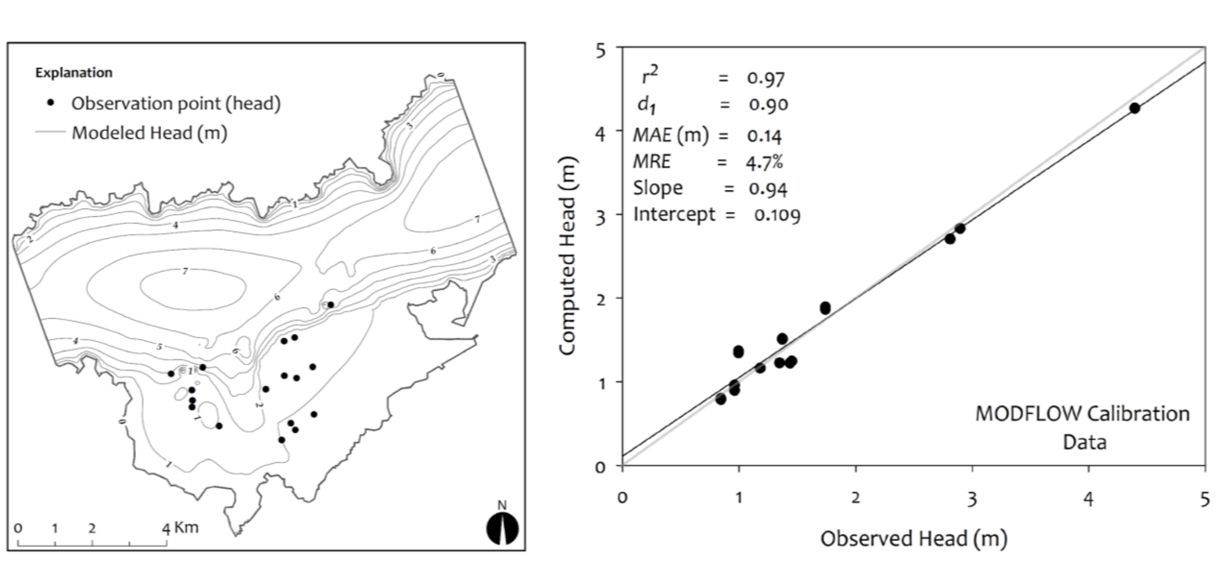

Fig. 6a (left). Observation points and computed heads from the MODFLOW model. 6b (right). Comparison of observed vs computed heads from the calibrated MODFLOW model. The *symbols* are: coefficient of determination (r^2), mean average error (*MAE*), mean relative error (*MRE*), and modified index of agreement (d_1). The *solid grey line* is the 1:1 line and the *solid black line* is the linear regression.

3.2.2 - Sensitivity analysis.

To address modeling uncertainty, a sensitivity analysis was performed for important model input parameters to determine how critical each was in affecting the models' performance. The parameters chosen for analysis were: horizontal hydraulic conductivity, recharge rate, longitudinal dispersivity, ratios of transverse to longitudinal dispersivity and vertical to longitudinal dispersivity, model run length, and N-attenuation coefficients. The relative magnitude of model sensitivity to each parameter was assessed with the following equation:

$$\nu_R = \frac{\Delta Mo/Mo}{\Delta Mi/Mi} \tag{2}$$

(McCuen & Snyder, 1986), where M_o and Mi are the model output and input parameters, respectively, ΔM_o and ΔM_i are the change in model output and input parameters, respectively, and ν_R is the dimensionless relative sensitivity coefficient. The magnitude of the sensitivity coefficient is a relative comparison of how much the model output changes based on equivalent changes in the various model input parameters, despite them having different physical units. The assessment measure chosen for the model output parameter was the *MAE* between observed and modeled TN concentrations. The variation in input parameters was standardized to an increase and a decrease of 50% of the initial value for each parameter. Of the seven tested parameters, changes in the attenuation coefficients had the greatest effect on the model outputs (Fig. 7).

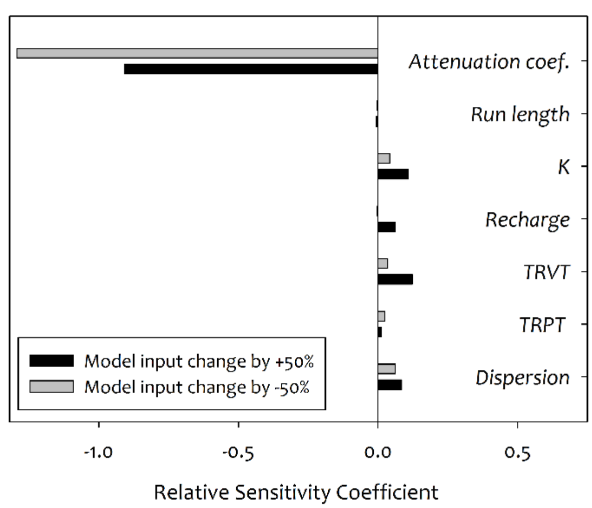

Fig. 7. Relative sensitivity coefficients between computed and observed TN concentrations, with respect to different input parameters for a ± 50% change in each parameter. Output parameter was chosen to be the mean average error (*MAE*).

3.2.3 - Attenuation factors and MT3DMS model calibration.

As stated earlier, to model the process of nitrogen attenuation in the vadose zone, an attenuation coefficient was applied to each type of modeled N, and the values of these coefficients were selected through model calibration. To select the best fitting set of coefficients, the results of the 5200 Monte Carlo model runs were filtered to only include those with sets of attenuation coefficients that produced computed versus observed slopes between 0.97 and 1.03 and intercepts between -3 and 3 µM. This subset was filtered to retain only the top 10% of the sets in regard to the mean absolute error (*MAE*). Finally, the single set of coefficients in this subset that yielded the highest correlation (d_1 and r^2) was chosen. The optimal attenuation coefficients were 0.44 for OSDS-N, 0.90 for piggery-N, and 0.48 for Agriculture-N. These factors compare reasonably well to previously measured rates of N-attenuation in other studies (Valiela et al., 1997; Almasri & Kaluarachchi, 2007; and others listed in Appendix B, Table B1). Once the MT3DMS model was calibrated with the best fitting set of attenuation coefficients, the resulting *MAE* of computed vs. observed TN values was 16.9 µM. The coefficient of determination ($\boldsymbol{r^2}$) and modified index of agreement ($\boldsymbol{d_1}$) were both 0.69, and the slope and intercept were calibrated to 0.97 and 3, respectively (Fig. 8).

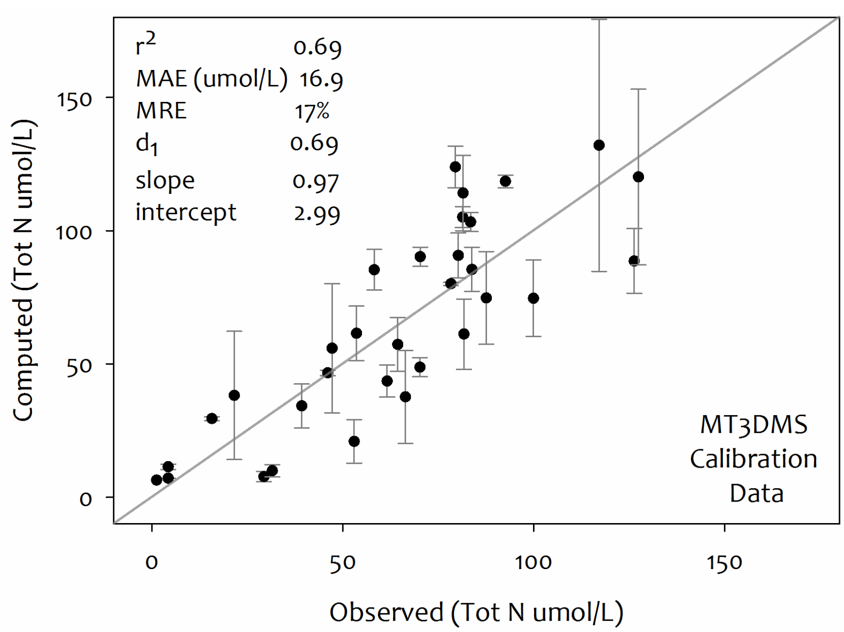

Fig. 8. Scatter plot of MT3DMS model calibration data based on observed vs. computed total N concentrations at observation points. The *solid grey line* is the 1:1 line. Each point represents the median computed value from all cells within 45 m of the actual sample location, and *error bars* represent the median absolute deviation (*MAD*) from these cells.

3.2.4 - Assessment of the influence from modeled N-sources.

Once calibrated, the MT3DMS model was used to estimate the relative TN contribution from each source throughout the model domain (Fig. 9). Modeled concentrations of all four N-types were summed to compare modeled TN values to measured TN values at wells and springs. In addition, the fractional contribution (or the %-influence) of TN from each source was calculated for each observation point (Fig. 10) and also for each hydrologic unit. To quantify these results across the whole plain, weighted averages of %-influence at all observation points were calculated, with weighting based on the relative concentration of TN in each model cell (Table 2). The weighted average indicated that 61% of the modeled TN originated from OSDS units, whereas only 15% originated from pigs, 13% originated from agriculture, and the remainder originated from natural soil sources. Since the model was assumed to be at steady state (inputs = outputs in each cell), the mass of TN in each cell could be calculated at the last time-step to represent the total mass of each N-type stored in the aquifer. Differences between model regions were also assessed by averaging the %-influence and stored N-mass across all cells in each hydrological unit (Table 2).

To assess confidence in the modeled %-influence values as well as uncertainty in the attenuation coefficients, %-influence values from each of the 5,200 Monte Carlo calibration runs were plotted against correlation-based and error-based metrics of model fit. This produced distributions that showed the model response to changes in attenuation coefficients, and also qualitatively helped to validate the calibrated values of %-influence. The model runs with sets of attenuation coefficients that produced a better model fit (e.g., error minimums and correlation maximums) also generally ended up producing similar fractions of %-influence from each of the four N-sources (Fig. 11). These regions-of-best-fit occurred when OSDS, piggery, and soil %-influence values centered on 60%, 17% and 10% respectively. The best-fitting agricultural %-influence values spanned a larger range between 10-20%.

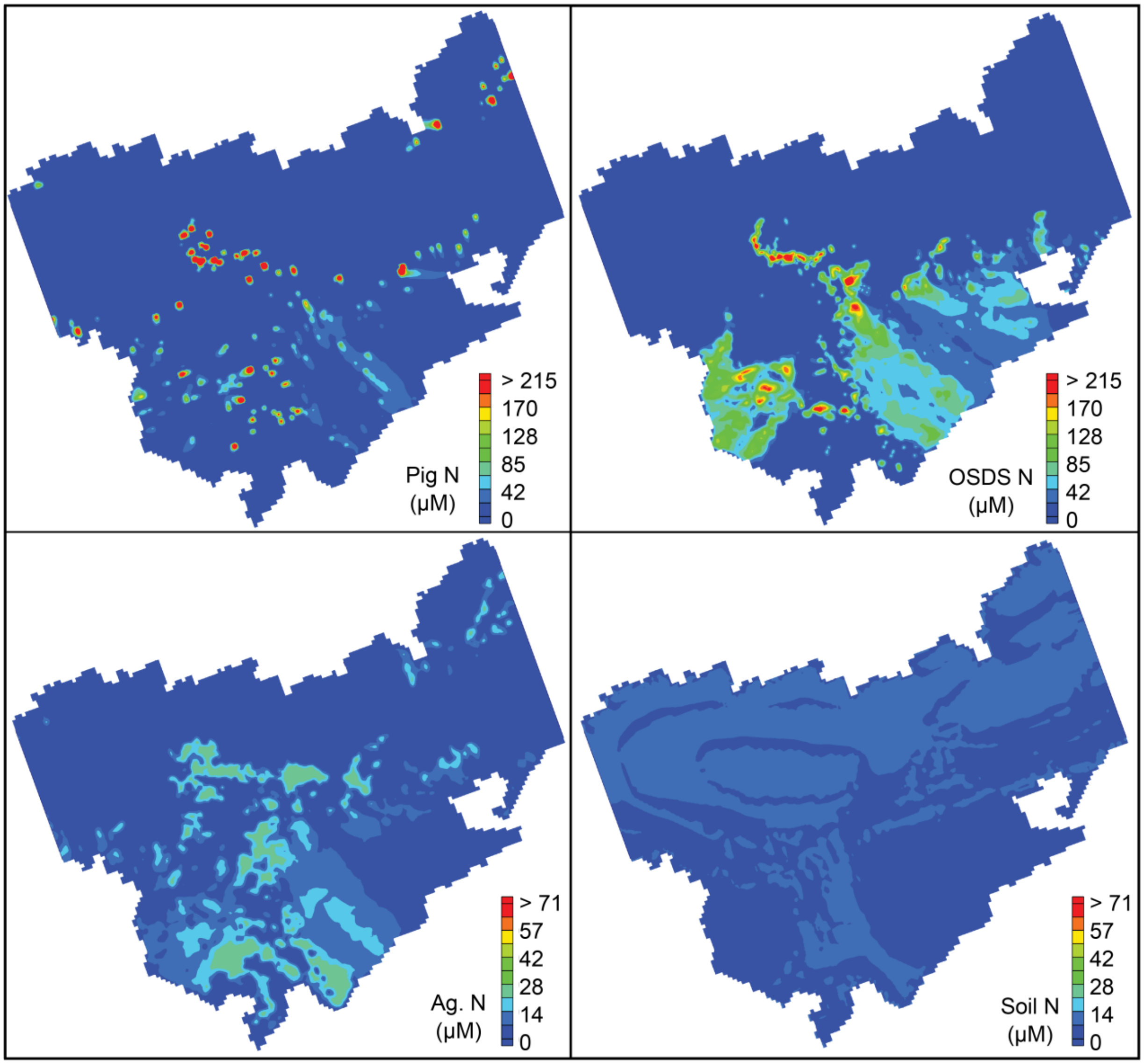

Fig. 92. The spatial distribution of N from each source at the end of the simulation period. Note different *scales of N concentration* for sources.

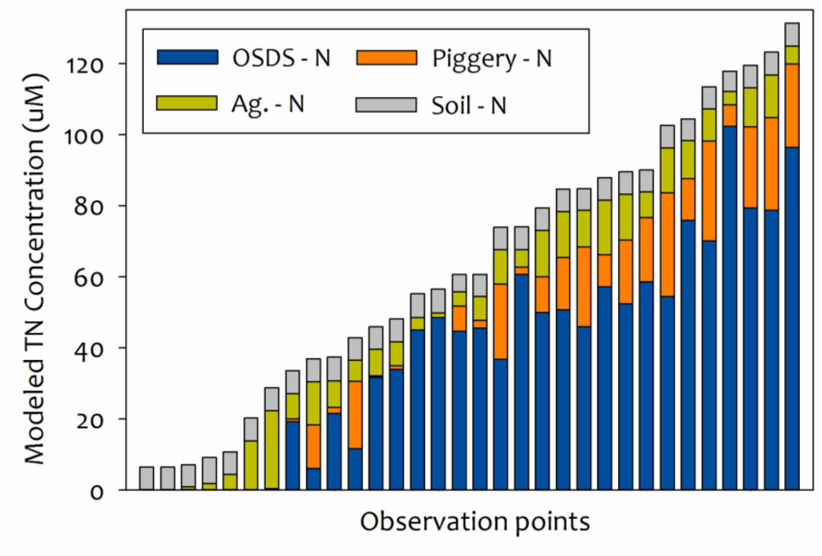

Fig. 10. Modeled concentrations at each of the 32 observation points (*represented by bars*). *Colors* represent the fractions of TN from each source.

Table 2. Modeled *percentages of influence* and total mass of stored TN in metric tons (numbers in parenthesis) from each N-source at observation points as well as average values from all cells in each hydrologic unit.

Hydrologic unit	Piggery N	OSDS N	Ag. N	Soil N
Concentration weighted averages from all cells in hydrologic unit				
Leone unit	*14%* (3.7)	*70%* (18.7)	*9%* (2.5)	*7%* (1.7)
Tafuna unit	*18%* (15.5)	*63%* (53.5)	*10%* (8.7)	*9%* (7.9)
Old-volcanic unit	*22%* (13.4)	*26%* (15.9)	*14%* (8.2)	*38%* (22.9)
Pyroclastic unit	*20%* (3.2)	*37%* (5.8)	*27%* (4.2)	*17%* (2.7)
All T-L Plain units	*17%* (22.4)	*61%* (78.1)	*12%* (15.4)	*10%* (12.3)
Entire domain	*19%* (35.8)	*50%* (94)	*12%* (23.5)	*19%* (35.2)
Concentration weighted averages from all observation points				
All observation points	***15%***	***61%***	***13%***	***11%***

Number of observation points (n) was 32

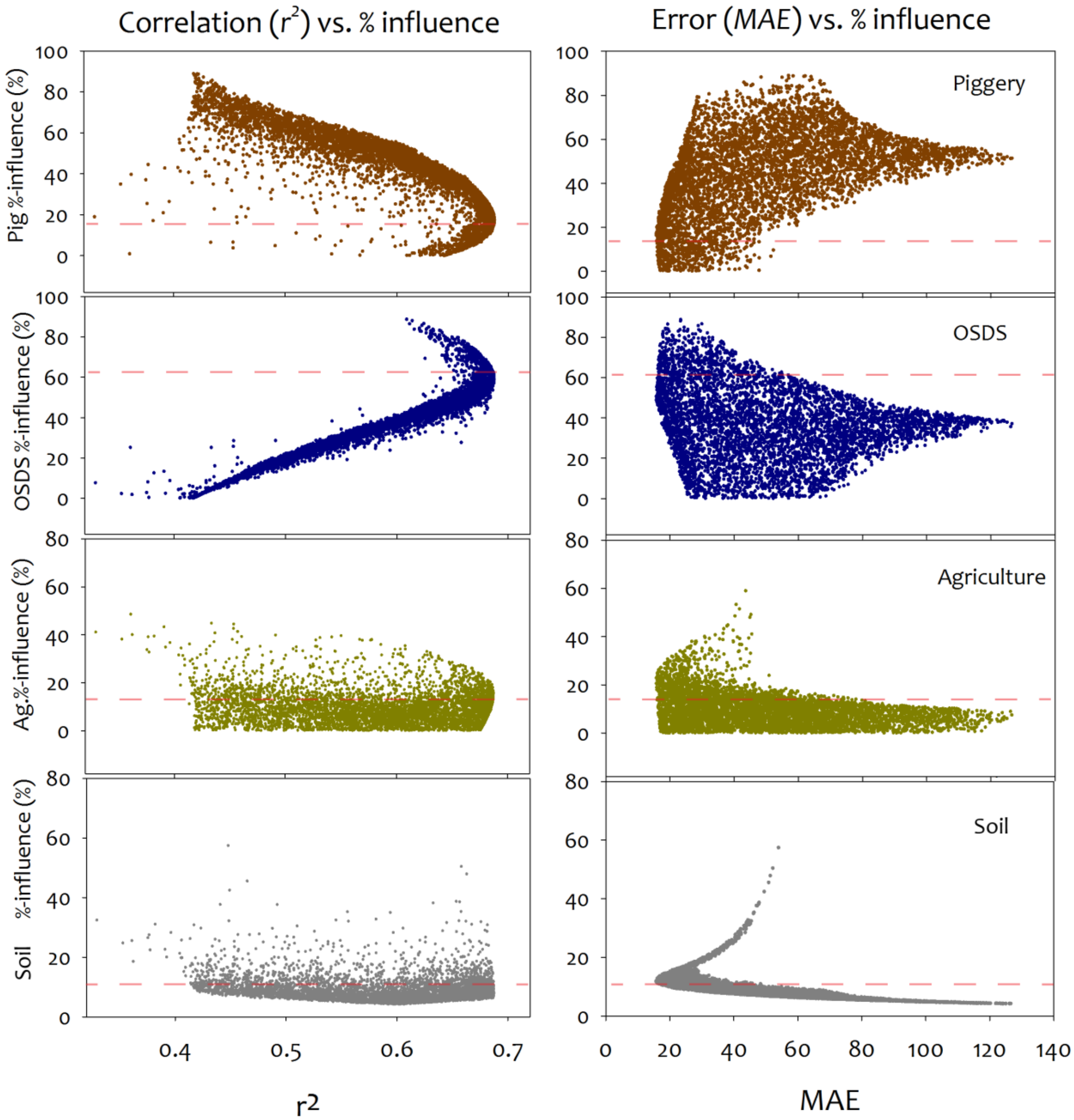

Fig. 11. Assessment of calibration uncertainty with Monte Carlo technique. Model fit metrics, r^2 and Mean Average Error (*MAE*) (in μM) are plotted against calculated percentages of influence from each of the four modeled N-sources. Each *point* represents a single model run with a randomly generated combination of N-attenuation coefficients. Error minima and correlation maxima occur with runs that output similar %-influence distributions. *Dashed red lines* indicate the %-influence values from the calibrated model (see table 2).

3.3 – MODEL VALIDATION WITH ISOTOPE MIXING MODEL

In groundwater settings influenced by multiple N-sources, observed $\delta^{15}N_{(NO3^-)}$ values at wells are primarily controlled by mixing, as long as NO_3^- acts conservatively within the aquifer. As stated previously, the groundwater N-sources in this region contribute NO_3^- as the primary form of TN, and they theoretically produce NO_3^- with distinctive and predictable $\delta^{15}N$ values. Under these assumptions, an isotope mass balance may be used to model mixing and to validate the MT3DMS derived fractional TN contributions from each source. A mass balance approach was therefore used to calculate a modeled $\delta^{15}N$ value for the NO_3^- at each of the observation points, which could be compared to the corresponding measured $\delta^{15}N$ value. The modeled $\delta^{15}N$ value is based on an estimated end-member $\delta^{15}N$ value of each source and the modeled fractional contribution from each of the four sources. This equation takes the form:

$$F_p \times \delta^{15}N_p + F_c \times \delta^{15}N_c + F_a \times \delta^{15}N_a + F_s \times \delta^{15}N_s = \delta^{15}N_{modeled} \qquad (3)$$

Where subscripts indicate the N-source: p = piggery, c = OSDS, a = agriculture, and s = soil, and:

F_x is the fraction of the simulated TN from each source x, computed at the observation point

$\delta^{15}N_x$ is the assumed end member $\delta^{15}N$ value of NO_3^- from each source where:

$\delta^{15}N_p$ = +15‰

$\delta^{15}N_c$ = +9‰

$\delta^{15}N_a$ = 0‰

$\delta^{15}N_s$ = +4‰

and

$\delta^{15}N_{modeled}$ is the final modeled $\delta^{15}N$ value of groundwater at the observation point.

The end member $\delta^{15}N$ values, listed above, are intermediate values selected from within documented ranges in the literature, as described below. Natural soil sources were assumed to primarily release NO_3^- from the breakdown of soil organic matter, as opposed to NO_3^- deposition in aerosols or rain, processes that are insignificantly small in American Samoa due to its distance from industrial N sources (Savoie et al., 1987). The published range for $\delta^{15}N$ of NO_3^-

in natural soils (+2‰ to +5‰) is usually slightly enriched relative to atmospheric sources, and the range of fertilizer influenced soils (-4‰ to +4 ‰) is generally near 0‰ (Kendall & McDonnell, 1998). Although manure and human wastewater have overlapping $\delta^{15}N$ ranges (+8‰ to+25‰), it has been suggested that septic systems may produce $\delta^{15}N$ values at the lower end of this range (+8 to +11‰), and animal manure may have higher values with more variability (+10 to +25‰) (Bohlke, 2003; French et al., 2012).

These end-member estimates were incorporated with the modeled source fractions in the mass balance and $\delta^{15}N_{modeled}$ values were compared to $\delta^{15}N_{measured}$ values with the aforementioned fit metrics. These yielded a *MAE* of 1.2‰ and an *MRE* of 19%. The coefficient of determination (***r***^{2}) was 0.59, the modified index of agreement (***d***$_1$) was 0.65, and the slope and intercept were 0.98 and 0.18‰, respectively (Fig. 12). This technique provides a way to validate and assess the MT3DMS model's reliability in predicting the contaminant fractions originating from each source, something that otherwise would not be possible to directly measure. Limitations of the approach and related uncertainties (discussed later) should be kept in mind, however.

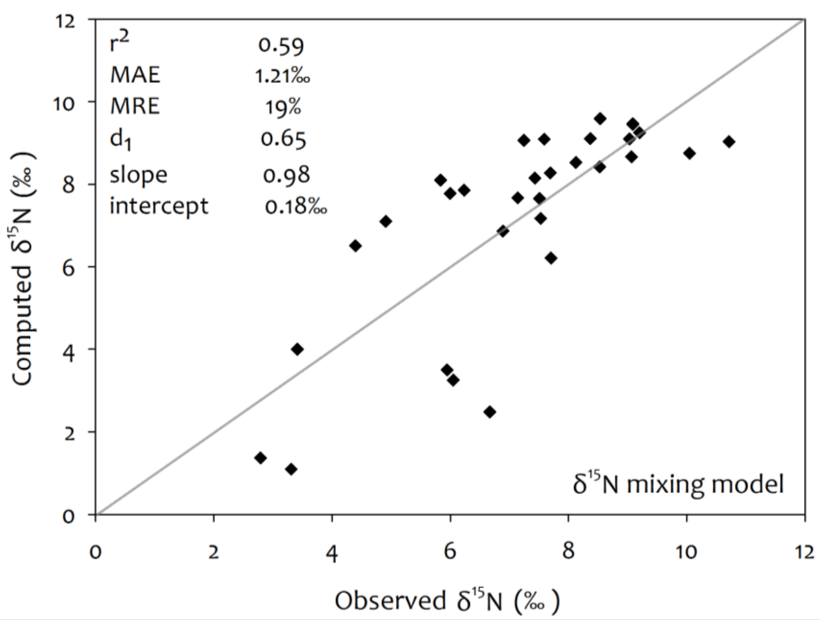

Fig. 12. Nitrogen isotope mixing model results showing comparison of model computed $\delta^{15}N$ values to measured $\delta^{15}N$ values from samples. The *solid grey line* represents the 1:1 line.

3.4 – LAND-USE AND MANAGEMENT CHANGE SCENARIOS.

Once the model was calibrated to reflect current conditions, land-use and management change scenarios were developed and applied to the N-loading model in order to predict different actions' effects on groundwater quality. Table 3 shows six different scenarios, two of which were developed with the assistance of local water resources stakeholders (AS-EPA and ASPA) to test the outcomes of projects that are likely to be considered.

Expansion of the existing sewer system to serve the western half of the Tafuna-Leone Plain has been proposed. To model this action, all OSDS units within 125 m of the major roads in the Western Plain were removed from the N-loading model, resulting in a reduction of 803 OSDS units. This reduced TN concentrations in Leone wells by more than 50%. Another scenario considered the efficacy of a fully centralized wastewater collection system by testing its antithesis: replacing all sewer-connected households with OSDS units. The results of this scenario indicate that without the existing wastewater collection system, total aquifer N-loading would be about 43% higher. Other scenarios included reduction of pig numbers, and increasing fertilizer application rates on agricultural lands. All scenario results were assessed by comparing changes in TN loading, aquifer TN storage (within the entire model domain), changes in %-influence distributions, and the change in the modeled TN concentrations at springs and production wells.

Table 3. Results of land-use and management change scenarios on TN loading, storage, and influence to groundwater

Scenario	Change factor	Δ TN loading (Mg/yr)	Δ TN storage in aquifer (Mg)	Δ TN storage in aquifer (%)	Average [TN] at wells (μM)	Pig TN %	OSDS TN %	Ag. TN %	Soil TN%
Addition of sewers along main roads in Leone	- 803 OSDS units	-3.7	-12.6	-6.4%	49*	20%	50%	16%	14%
Increased OSDS efficiency by 25%	OSDS N attenuation increased to 69%	-6.8	-42.0	-22.3	47.3	20%	48%	18%	14%
Removal of all sewers and conversion to OSDS	+ 2471 OSDS units	+11.5	+69.7	+37%	121**	13%	69%	10%	8%
Reduction in Pigs by 50%	**-** 1680 pigs	-2.3	-17.8	-9.5%	61.5	8%	66%	14%	12%
Pig manure agricultural use program	-2520 pigs & -50% Ag inputs	-2.3	-26.2	-13.9%	57.6	4%	67%	17%	12%
Increase in agricultural applications by 2x	+ 2.8 kg-N/ ha/yr	+2.4	+23.5	+12.5%	75	13%	54%	23%	10%
	-	**Initial TN loading**	**Initial TN storage**	-	**Initial [TN] at wells**	**Initial %-influence values**			
Initial state	-	**26.8**	**188.5**	-	**66**	**15%**	**61%**	**13%**	**11%**

Δ TN loading reflects N that has been attenuated at calibrated attenuation rates, in metric tons (Mg)

** Leone wells only. Initial average [TN] = 109 uM*

*** Tafuna wells only. Initial average [TN] = 77 uM*

4. DISCUSSION

4.1 – RESOURCE MANAGEMENT IMPLICATIONS

The results shown in Table 2 indicate that wastewater management should be a high priority for reducing the contamination vulnerability of Tutuila's drinking water supply. Since generating human waste is unavoidable, reduction of wastewater discharge on Tutuila could be accomplished by either installing wastewater collection systems (sewers) or replacing cesspools and inefficient septic tanks with higher efficiency OSDS units. Either of these actions on a wide enough scale should result in a significant reduction of groundwater N, and by inference, other wastewater related contaminants. Management actions regarding piggeries or agriculture may also serve to reduce contamination vulnerability somewhat, and the relatively smaller scales of these activities may make effective management easier to enact. Assessing the efficacy of these or other actions by running land-use change scenarios with the model presented in this study may be useful for management planning efforts.

The model can also be used for obtaining a general, though indirect, estimate of TN attenuation rates affecting the three modeled N-sources on the island. Although, it must be noted that these attenuation rates are more uncertain than rates derived from a dedicated N-attenuation model, since they were derived via calibration and not empirical observations. Regardless, the magnitude of the calibrated N-attenuation factors, at least qualitatively, can highlight important issues. For example, the modeled agricultural attenuation rate of 48% indicates that less than half of all applied fertilizers are used by plants (or are lost in other ways), whereas the other half ends up leaching to the aquifer. This suggests that in general, synthetic fertilizers are being over-applied on Tutuila. Although agricultural inputs are not the island's most significant contributors of groundwater TN, this result nonetheless indicates potential for groundwater contamination, should there be a widespread increase in fertilizer application. This underscores the importance of developing agricultural regulations, permitting requirements, and management practices in a rapidly developing setting such as Tutuila. An important step in agricultural management on Tutuila would be to develop a more detailed inventory of agricultural areas and rates of fertilizer, pesticide, and herbicide applications. A higher resolution agricultural dataset could be used with this modeling framework to provide a more reliable assessment of fertilizer fate and agriculturally sourced water quality issues.

In this study, piggery-sourced groundwater contamination was shown to be less important than many previous studies have suggested (Falkland, 2002; AS-EPA, 2005). However, pig manure's effects on groundwater quality are probably secondary to its effects on surface water quality. In contrast to OSDS wastewater, which is essentially injected into the subsurface, pig manure is generally discharged directly to the ground's surface making it more likely to be removed by surface runoff. The higher modeled attenuation coefficient (90%) for pig nitrogen supports this conclusion. Assessment of the efficacy of piggery management efforts should therefore focus on surface water quality as opposed to groundwater quality.

4.2 - MODEL VALIDITY AND LIMITATIONS

Assessing the validity of this model's results requires determining how well the MT3DMS model predicts the fraction of impact from each source. Here, this was accomplished by using a $\delta^{15}N$ mixing model and comparing its results against measured nitrogen isotope data. This method relied on identifying a distinctive end member $\delta^{15}N$ value for each of the mixed N-sources. However, in reality, the N-source end-members probably span a range of $\delta^{15}N$ values due to variable degrees of fractionation throughout the evolution of N from individual locales. This concern is commonly brought up in other studies that use isotopic values for source discrimination (Kendall & McDonnell, 1998; Ransom, 2015). For example, overlapping $\delta^{15}N$ ranges from manure and OSDS $\delta^{15}N$ are an important concern, but in this study, the simplifying assumption that each has a unique endmember value was made. The validity of this assumption remains a subject of debate, so for this study, ancillary information regarding the magnitude of impact from these two sources was also explored to better understand pig manure's potential to be a significant factor in the observed high groundwater $\delta^{15}N$ values.

This was accomplished by comparing historical water quality and pig census data from the last decade. Piggery data shows a clear decline, of about 38%, in the number of pigs on the island over the last 10 years (AS-EPA, 2005; AS-EPA, 2013). If pigs were a significant source of groundwater nitrogen, a reduction of this scale would be expected to diminish nitrogen concentrations by a measurable amount, considering the plain's relatively rapid groundwater movement. However, average NO_3^- concentrations taken from sixteen Tafuna-Leone wells during annual US-EPA drinking water quality compliance testing do not follow a similar trend (Fig. 13). Instead, NO_3^- values in groundwater averaged around 50 μM between 2005 and 2015 and did not show a significant change over this time period. This supports the conclusion that high TN and $\delta^{15}N$ groundwater is more likely to be impacted by OSDS rather than piggeries, since pigs do not seem to be major nitrogen contributors to groundwater.

The mixing model validation approach also relies on the assumption that $\delta^{15}N$ values of NO_3^- and of TN in Tutuila's groundwater are equivalent, since the model uses TN values but the $\delta^{15}N$ analysis only measures $\delta^{15}N_{(NO3-)}$. This discrepancy was accepted because T-L Plain groundwater is generally well oxygenated, and thus, about 90% of TN is in the oxidized form of NO_3^-. Generally high groundwater DO concentrations also suggest that denitrification is not likely to be a significant process within the aquifer. The process of denitrification is a biologically mediated N-attenuation process that occurs in anoxic environments. It modifies $\delta^{15}N$ values and reduces TN concentrations as water flows through the saturated zone. However, on Tutuila, groundwater is well oxygenated, TN concentrations generally increase down groundwater flow-paths, and there are low concentrations of total organic carbon (a fuel supply for denitrifiers) in the subsurface. These pieces of evidence imply that TN acts and moves conservatively while in the aquifer, and denitrification is not a significant process affecting TN concentrations or $\delta^{15}N$ signatures.

The modeling approach also relies on a key assumption that both the model itself and that real-world physical parameters, such as hydrologic and climactic conditions, are in a steady state during the modeled period. Repeat sampling results from multiple years and climate data from the last decade was examined to justify this assumption for physical parameters. To test the steady state assumption in the model, the simulation was run for various lengths of time. Error and correlation based fit metrics fluctuated at short time-steps, but then stabilized after about 8 years (Fig. 14). The final model was run for an 80-year duration to ensure steady state conditions.

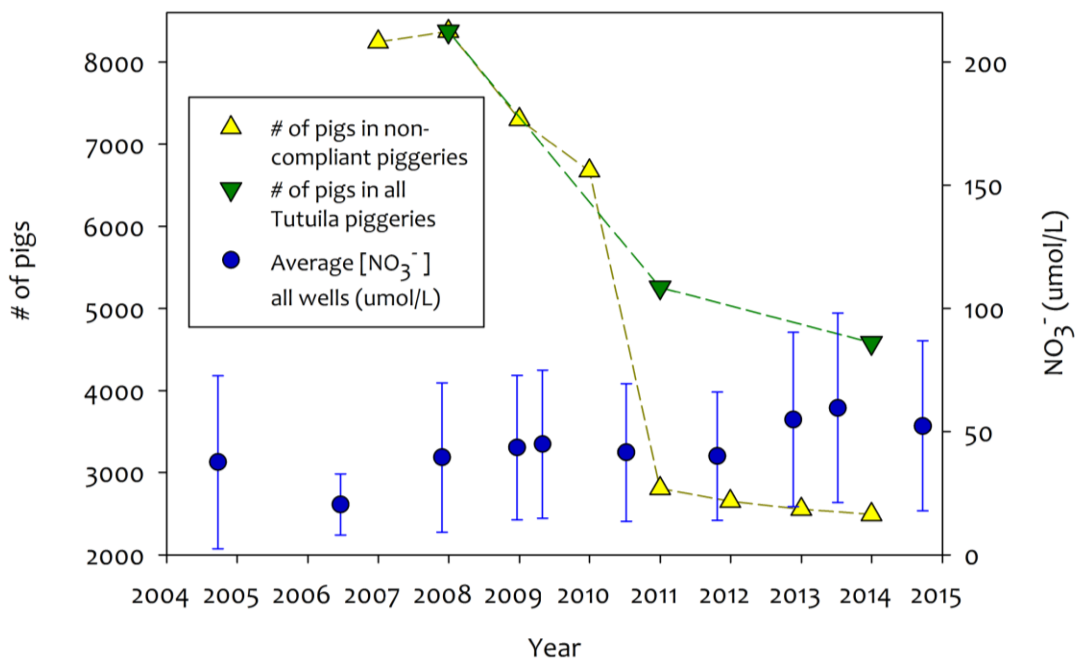

Fig. 13. Comparison of trends in pig numbers from AS-EPA pig census information (*yellow and green triangles*) and nitrate + nitrite concentrations from annual routine water quality sampling data averaged across sixteen Tafuna-Leone wells (*blue points*).

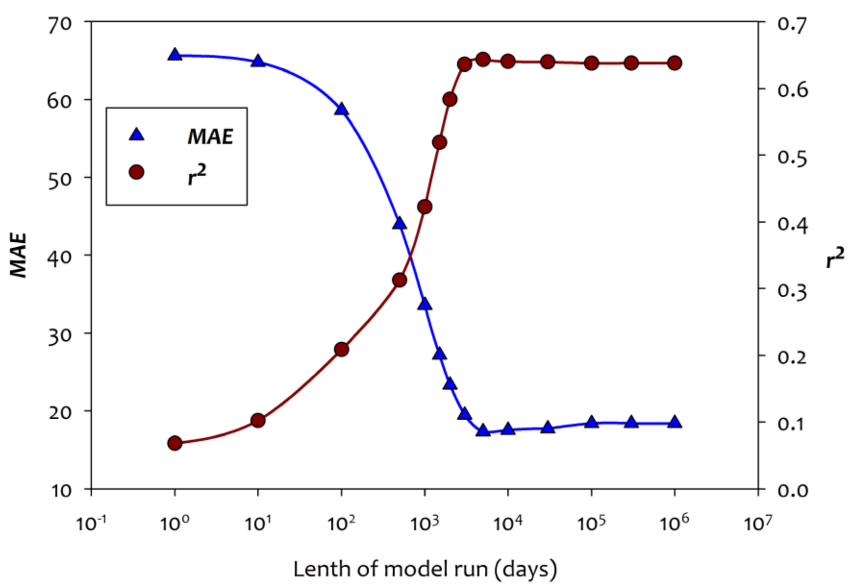

Fig. 14. Assessment of steady state conditions in the MT3DMS model via comparison of run length against Mean Average Error (*MAE*).

4.2.2 - Limitations and Assumptions

In this study, data form multiple sources and of varying quality was compiled into a single framework. Assumptions and uncertainties from the model codes themselves and from input data sets are propagated through this framework. Although it is unrealistic to directly quantify these uncertainties, they should nonetheless be considered when interpreting model results. Important assumptions that are implicit in the results include the following:

1) It is assumed that nitrogen acts conservatively within the saturated zone, and all vadose zone attenuation processes are accounted for with the attenuation coefficients.

2) Land-use datasets came from different sources and assessing their accuracy was not always possible. Every effort was made to utilize data of the highest available quality.

3) The study's significance relies on the assumption that TN is predictive of human impact, and may be correlated with other potentially harmful contaminants from the modeled sources.

4) The conceptual geological model used in this study assumes the overall conductivity of the subsurface can be adequately represented by a limited number of K values. Although borehole logs indicate the subsurface structure of the T-L Plain is far more convoluted, data availability limits the geologic complexity that can be modeled with certainty.

5) Observation points are unevenly distributed, and more numerous on flat terrain. Steeper terrain is underrepresented in the observation point network due to a lack of wells in those areas. Despite this limitation, most of the N-sources and areas of interest are proximal to the observation points. Steeper areas were included in the model primarily to provide more accurate boundary conditions to the Tafuna-Leone Plain.

6) Natural soil sources of N were only measured in up-gradient locations, assumed to be small, and also assumed to be homogeneously distributed. Possible heterogeneity in wild animal populations (e.g., fruit bats or pigs) was not considered.

7) The attenuation coefficients are parameterized values based on model calibration. This study does not aim to directly quantify attenuation rates and these values should be taken as general estimates only.

4.3 - LOCAL AND REGIONAL SIGNIFICANCE

This study illustrates the fact that anthropogenic activities directly and quantifiably affect Tutuila's groundwater quality. Unregulated development and use of low-efficiency wastewater management systems is a clear threat to the sustainability of water resources in American Samoa. Although these issues have so far remained unresolved, high recharge rates and short groundwater transit times (Izuka et al., 2007) give hope for reasonably fast recovery and remediation once management efforts are applied. Problems with existing wells on Tutuila have encouraged an increased rate of water development on the island, and it is important that new wells are located in areas with low contamination vulnerability. Water authorities exploring for new well sites on Tutuila may find these model results very useful, as the framework incorporates multiple water quality and hydrogeological datasets that are generally helpful for locating sustainable groundwater development sites. Land-use managers may also find these results useful for delineation of water protection regions, or special management areas.

The modeling framework presented in this study not only enables land-use managers to assess groundwater contamination vulnerability on Tutuila, but also serves to advance our understanding of non-point source contamination in other tropical island settings. The framework used here is applicable on islands where multiple co-linearly distributed N-sources and complex volcanic geology interact to create convoluted geochemical signals. This study shows that Tutuila's multiple contamination sources all have a measurable effect on groundwater quality, however these effects clearly do not have equal magnitudes. The quantification of pollutants from multiple sources is a problem for many island nations, and applying source dependent tracers, such as $\delta^{15}N$, within a groundwater modeling framework lends additional confidence to the results of both techniques. The management implications for applying this tool are believed to be significant. By distilling multiple complicated datasets into a simple prioritization matrix, this framework provides simple, quantitative, and reasonably validated results that are easily communicated to resource management agencies and to the public. This information can be used on Tutuila or elsewhere to assist in making management decisions or to increase public support for sewer projects or proposed modifications in agricultural practices.

5. Conclusions

Like many small islands that rely on groundwater resources, Tutuila's drinking water is vulnerable to contamination from three predominant non-point pollution sources: OSDS sourced wastewater, agricultural chemicals, and livestock (pig) manure. Elevated levels of groundwater nitrogen in areas of human influence suggest the suitability of using dissolved TN as a tracer of anthropogenic water quality impacts. In this study, land-use data and hydrological parameters were integrated to develop a multi-species contaminant transport modeling framework intended to quantify and partition these impacts. The spatial distribution of TN in Tutuila's groundwater was found to be heterogeneous and primarily dependent on the prevalence of non-point sources located up gradient from the point of observation. By estimating the locations and TN contributions of these sources, the model was able to explain almost 70% of the observed variability in groundwater N concentrations. Results indicate that OSDS have a much larger influence on groundwater quality than do piggeries or agricultural practices. Quantitative ranking of sources was validated with a Monte Carlo based optimization method, which clearly showed model error minima and correlation maxima at average %-influence values of 61%, 15%, 13%, and 11% from OSDS, pigs, agriculture and soil sources, respectively. The reliability of the model predictions was validated with an isotope mixing model, which provided a way to assess the modeled N-fractions based on measured $\delta^{15}N$ values. Additionally, these results were supported by examining historical water quality and land-use data, which showed stable average concentrations of NO_3^- in production wells despite sharp declines in piggery numbers over the last decade. The calibrated model was then used to quantify the effects of hypothetical resource management scenarios on groundwater quality. This modeling framework serves as an example for source partitioning of co-linearly distributed non-point sources of contamination, on small tropical islands, to aid in the design of best management practices.

APPENDIX A:
OBSERVATION POINT SELECTION METHODS

A.1 - MODFLOW observation points.

The MODFLOW model was re-calibrated with static water levels from 17 observation points taken during a synoptic water level survey in 2014 (Appendix C, Table C1). Recovery tests were performed on each well and once the wells were fully recovered (usually 4 to 24 hours) the water level was recorded. Since wells in the ASPA system are almost always pumping, the measured water levels did not actually represent normal steady state conditions at the measured locations because drawdown effects were almost always present. To account for this, the measured water level was instead assigned to a point near the well and on the same equipotential contour line, but outside of the well's estimated cone of depression. These 'hypothetical observation points' were assumed to have the same water levels as those in the stopped wells, but during normal pumping conditions. The hypothetical observation points were located at the intersection of the outer edge of the well's cone of depression and the equipotential line in the regional groundwater flow field (Fig. A1). The regional flow field was estimated from the Izuka et al. (2007) model, and the cone of depression was estimated based on the well discharge and the recharge rate around the well (Todd & Mays, 2005).

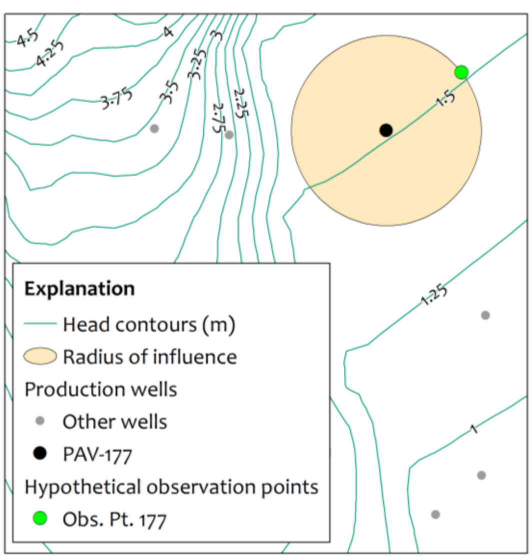

Fig. A1. Example of the geometry for assigning hypothetical MODFLOW head-level observation point locations based on the radius of influence and the regional groundwater potentiometric surface.

A.2 - MT3DMS observation points.

Measured TN values from water samples were incorporated into the MT3DMS model as observation points. It was found that observation points whose locations were arbitrarily close to a cell boundary were not able to represent the sharp modeled concentration gradients between adjacent cells, because the MT3DMS model computed TN concentrations at the center of each cell, regardless of where the actual location of the observation point fell. To compensate for this, the observation point was assigned the median TN value of all cells that fell within a 45 m radius (one half of the cell width) from the actual well or spring location. This method produced simulated TN concentrations that better approximated the observed data.

APPENDIX B:
SUPPLEMENTARY INFORMATION

B.1 - Calibration Assessment Measures

Model performance is typically assessed by comparing observed values of a parameter against the corresponding modeled values. Correlation-based and error-based statistical measures are commonly used to assess the model fit (Almasri & Kaluarachchi, 2007). Though there are many approaches that are appropriate for this purpose, in this study, the following measures were selected as metrics of model performance: 1) the coefficient of determination (r^2), 2) the least mean squares regression coefficients (*slope and intercept*), 3) the modified index of agreement (d_1), 4) the mean average error (*MAE*), and 5) the mean relative error (*MRE*).

The modified index of agreement (d_1) is a correlation based measure and is defined by:

$$d_1 = 1 - \frac{\sum_{i=1}^{n}|Oi - Si|}{\sum_{i=1}^{n}(|Si - \bar{O}| + |Oi - \bar{O}|)} \tag{B1}$$

(Legates and McCabe, 1999), where n is the number of observations, O_i is the measured value at observation point i, and S_i is the corresponding modeled value at point i. The value of d_1 ranges from 0 to 1 with higher values representing better model fit. This metric is similar to the coefficient of determination (r^2). However, while r^2 describes how much of the total variance within the observed values can be explained by the model, it only quantifies the relative dispersion in the data and does not account for systematic over or under predictions. The modified index of agreement (d_1) represents the ratio of the mean square error and the potential error, which is intended to overcome the insensitivity of r^2 to systematic errors. Additionally, the slope and intercept of the observed vs. simulated LMS regression are also useful indicators of systematic over or under predictions (Krause et al., 2005).

The error-based measures used in this study assess goodness-of-fit based on quantifying the differences between observed and modeled values. They include the mean absolute error (*MAE*) and the mean relative error (*MRE*), which are described by:

$$MAE = \frac{\sum_{i}^{n}|Oi - Si|}{n} \tag{B2}$$

and

$$MRE = \sqrt{\frac{\sum_i^n (Oi - Si)^2}{n}} \times \frac{1}{\Delta} \qquad \text{(B3)}$$

(Anderson and Woessner, 1992; Almasri & Kaluarachchi, 2007), where Δ is the range between the highest and lowest values in the observed data. These metrics both represent the average of all errors between observed and modeled points. However the *MRE* is normalized to the dataset, and is thus expressed as a percentage.

B.2 - Previously measured rates of N attenuation

Table B1. Published and calibrated attenuation estimates (this study) of N from anthropogenic land-use sources

Source	N-losses	Citation	Processes accounted for
OSDS	7-15%	(Van Cuyk et al., 2001)	all losses
	10-20%	(Siegrist et al., 2000)	volatilization, removal, denitrification
	25%	(Morgan et al., 2007)	volatilization only
	10-30%	(Hinkle et. al., 2008)	volatilization only
	90%	(CHEC, 2003)	all losses
	44%	**Calibrated value**	**all losses**
Pig Manure	47-56%	(Lee et al., 2011)	volatilization only (cattle manure)
	51-63%	(Viers et al., 2012)	volatilization only
	10-99%	(Choudhary et al., 1996)	all losses (depending on treatment)
	90%	**Calibrated value**	**all losses**
Synthetic Fertilizers	18%	(Bouwman et al., 2002)	volatilization only
	48%	(Viers et al., 2012)	volatilization, runoff, harvest
	50%	(Bohl et al., 2001)	denitrification, surface runoff, leaching to groundwater
	48%	**Calibrated value**	**all losses**

B.3 – Watershed population density vs. TN concentrations in groundwater

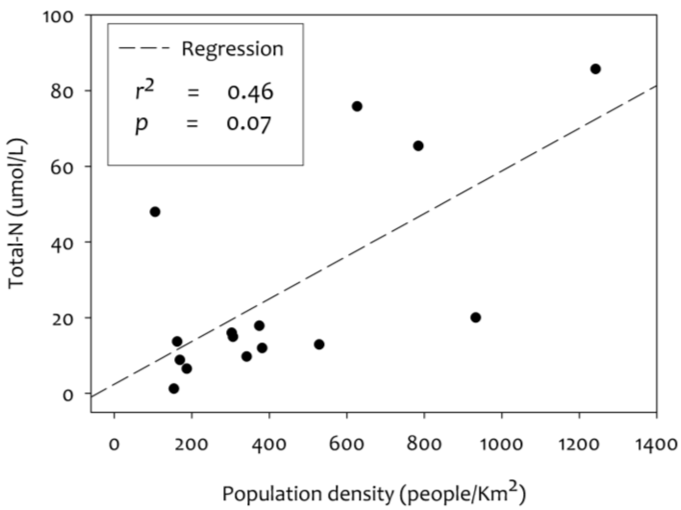

Fig. B1. Averaged concentrations of TN from groundwater samples vs. population density in Tutuila's watersheds. Sample values are from 2013 sampling campaign, and population estimates are from 2010 census data.

B.4 – Details of modifications for land-use and management change scenarios

Addition of wastewater collection area in Leone:

Expansion of the existing sewer system to serve the Leone side of the Tafuna-Leone Plain has been proposed by the by the American Samoa Power Authority (ASPA). In this scenario all OSDS units within 125 m of the major roads in the Western Plain were removed from the N-loading model, resulting in a reduction of 803 units (Fig. B2). It was assumed that sewer mains are likely to be built following the main roads and that connections may be extended up to 125 m (≈400 ft.) from the main line. This model could be modified to reflect specific designs once proposed construction plans are available.

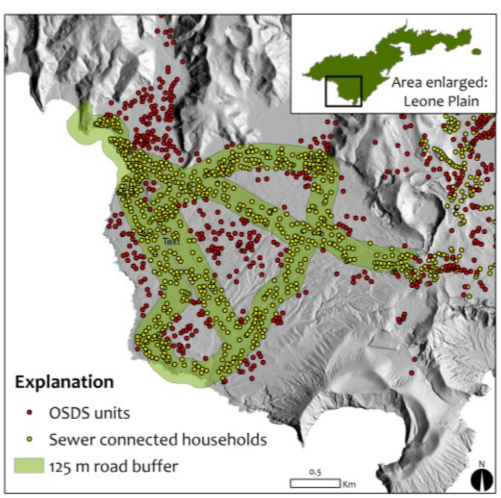

Fig. B2. Locations of OSDS units outside of (*red dots*) and inside of (*yellow dots*) the hypothetical Leone-Wastewater- Collection Zone (*green shaded area*).

Removal of all sewers and conversion to OSDS

The efficiency of the existing centralized wastewater collection system in reducing groundwater TN was also tested (Fig. B3). This was accomplished by modeling all sewer-connected households as OSDS units. This resulted in an increase of 2,471 OSDS units, which nearly doubled the OSDS loading in the model. Since the existing collection system is primarily located on the Tafuna side of the Tafuna-Leone Plain, effects of the additional loading were concentrated in this region. The results of this scenario clearly show that the existing sewer system is providing a substantial benefit to the island.

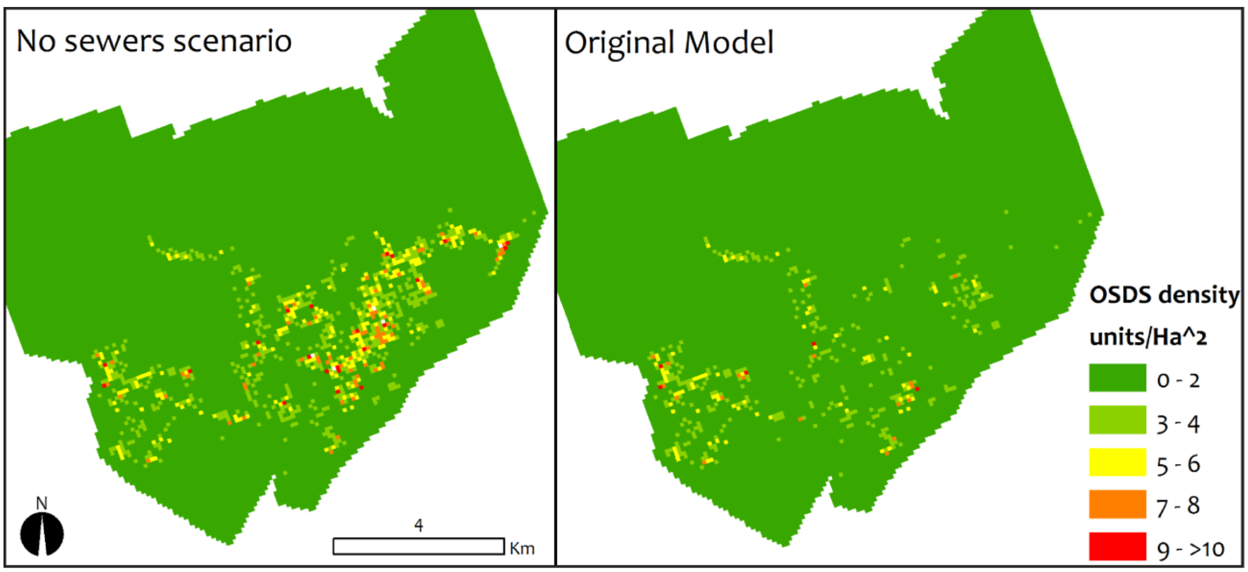

Fig. B3. Comparison of OSDS density in the original N-loading model (right) to OSDS density in the hypothetical scenario (left) where all households currently connected to sewers are placed on OSDS units.

Increased OSDS efficiency by 25%

Following input from ASPA representatives, this scenario was developed to explore a potential technological solution for reducing OSDS sourced nutrients and other contaminants. Representatives from ASPA are considering a replacement program that would convert low-efficiency OSDS units to ones that may utilize engineered percolation media. Higher efficiency OSDS units designed and installed by ASPA may be able to achieve nitrogen and/or other contaminant attenuation in packed beds directly below the units. A hypothetical increase of 25% was applied to the OSDS attenuation rate (for a final value of 69% attenuation) in the model to simulate the potential increase in attenuation that such a strategy may produce. As of this writing, research into the design and efficiency of these units is underway on Tutuila, and the results of these trials will be able to better inform further studies with this or other models.

Reduction in Pigs by 50%

Since 2006, the Piggery Compliance Program, which was initiated by the American Samoa Environmental Protection Agency (AS-EPA), has successfully reduced the number of pigs on Tutuila by over 50%. This scenario explored the potential groundwater quality effects if a similar reduction were to again occur in the future. In this scenario it was assumed that the spatial distribution of piggeries would not change, only that the number of pigs in each piggery would be halved. This decreased the number of pigs in the N-loading model by 1,680.

Increase in agricultural applications by 2x:

More and more farmers are said to be using synthetic pesticides and fertilizers on Tutuila. This scenario explored the effects of a potential increase in fertilizer use. The existing loading rate of agriculturally derived N was doubled, while keeping the same spatial distribution of agricultural areas. This action resulted in an additional application of 2.8 kg of N per hectare, per year, which is equivalent to total increase of 4.6 Mg of N per year applied over the entire model domain. After attenuation, N-loading to groundwater resulted in in an additional of 2.8 Mg of N per year.

Piggery waste composting and optimization

The AS-EPA is interested in promoting efficient use of piggery waste on the island. Representatives from AS-EPA helped to develop a scenario that tests the effects of a management initiative which would be designed to encourage farmers to use compost from piggeries to replace synthetic fertilizers. An initiative of this type would ideally reduce fertilizer consumption, while at the same time addressing problems related to animal waste. In this scenario, the loading model was modified to reduce piggery N-loading by 75% (9.6kg/day, after 90% attenuation), while maintaining the same spatial distribution of piggeries. The scenario assumed that this reduced fraction of pig waste was composted, and during this process was subject to an attenuation rate of 90%. The model assumed that the compost was then transported to agricultural areas where it was distributed evenly throughout existing agricultural land-use areas, resulting in an increase in agricultural N (manure) by 9.6kg/day. Plants theoretically absorbed and attenuated the manure-N at the same rate as synthetic fertilizer-N. Because crop yields were partially supported with nutrients from manure, it was assumed that farmers would use less synthetic fertilizer. The scenario also included a 50% reduction in synthetic fertilizer use, which was accounted for by reducing Ag. N-loading by 6.3 kg/day evenly across all agricultural land-use areas (scenario results are presented in Table 2).

APPENDIX C: ADDITIONAL DATA

Table C1. Measured water levels from production wells

Observation Point Name	Water Level (m above MSL)	Latitude	Longitude
Ili'ili Well Field			
Iliili-62-E	0.96	-14.346216	-170.746214
Iliili-62-W	0.96	-14.350319	-170.748472
Iliili-84-E	0.84	-14.344092	-170.740418
Iliili-84-W	0.84	-14.347848	-170.745102
Pava'ia'i Well Field			
Tafuna-177-E	1.37	-14.334663	-170.747873
Tafuna-177-W	1.37	-14.337963	-170.752473
Tafuna-171-E	1.02	-14.332489	-170.740789
Tafuna-171-W	1.02	-14.335213	-170.744798
Lower Malaeloa Well Field			
Malaeloa-93	1.45	-14.342342	-170.770872
Malaeloa-119	1.35	-14.346932	-170.764137
Malaeloa-91	1.44	-14.340678	-170.770808
Malaeloa-70	1.18	-14.338161	-170.770932
Upper Malaeloa Well Field			
Malaeloa-168	2.81	-14.332608	-170.768214
Malaeloa-169	2.89	-14.334231	-170.776091
Malaeimi Well Field			
Malaeimi-89	4.4	-14.317366	-170.736253
Mesepa-85-E	1.74	-14.325303	-170.745277
Mesepa-85-W	1.74	-14.326211	-170.747896

Table C2. Additional geochemical data from water samples

Name	Type	n	Latitude	Longitude	Salinity [a.]	DO [a.] (mg/L)	NO_3^- [b.] (μM)	NO_2^- [c.] (μM)	NH_4^+ [d.] (μM)	PO_4^{3-} [e.] (μM)	SiO_4^{4-} [f.] (μM)	TN [g.] (μM)	TP [h.] (μM)	TOC [i.] (μM)	$\delta^{15}N_{(NO3-)}$ [j.] (‰)
Iliili-62	Well	1	-14.34761	-170.74863	0.4	5.6	65.4	0.000	0.00	2.6	707.2	70.2	2.3	24.2	8.1
Iliili-76	Well	1	-14.34646	-170.74725	0.3	6.9	57.2	0.000	0.20	1.7	658.7	58.2	1.5	37.5	7.7
Iliili-84	Well	10	-14.34597	-170.74276	1.0 ± 0.1	5.3 ± 0.8	69.1 ± 13.9	0.002 ± 0.005	0.04 ± 0.06	2.2 ± 0.2	687.4 ± 30.7	78.3 ± 6.5	2.2 ± 0.4	20.3 ± 9.3	6.2 ± 0.2
Iliili-167	Well	1	-14.34178	-170.74714	0.3	7.0	119.7	0.003	0.00	3.3	941.5	126.3	3.0	11.7	7.5
Leone-70	Well	1	-14.33971	-170.77473	0.1	6.5	117.9	0.003	0.10	4.4	731.1	117.1	4.3	36.7	9.1
Leone -80	Well	1	-14.33889	-170.77324	0.1	7.4	88.4	0.000	0.00	4.6	685.5	87.6	4.5	15.8	5.8
Leone -83	Well	1	-14.336	-170.76941	0.1	7.3	58.2	0.014	0.00	2.8	732.7	66.4	2.6	8.3	4.9
Leone -91	Well	1	-14.34232	-170.76744	0.2	6.4	122.0	0.001	0.00	4.2	740.7	127.4	4.0	19.2	10.7
Leone -93	Well	10	-14.34348	-170.76787	0.2 ± 0.0	6.6 ± 0.9	68.5 ± 7.6	0.002 ± 0.004	0.12 ± 0.17	3.1 ± 0.6	723.9 ± 43.2	83.4 ± 17.7	3.0 ± 0.6	24.2 ± 8.7	9.2 ± 0.6
Leone -119	Well	2	-14.34596	-170.76707	0.3 ± 0.1	5.5 ± 0.1	74.6 ± 8.1	0.00 ± 0.00	0.045 ± 0.05	1.6 ± 0.6	687.4 ± 9.7	81.5 ± 5.0	1.4 ± 0.5	22.1 ± 7.7	9.1 ± 2.2
Malaeimi-67	Well	1	-14.31895	-170.73769	0.1	5.2	54.7	0.000	0.00	1.5	637.3	64.4	1.4	11.7	7.4
Malaeimi-85	Well	1	-14.3258	-170.74657	0.1	7.3	52.9	0.006	0.00	3.0	627.7	61.6	2.9	10.8	8.5
Malaeimi-89	Well	10	-14.31754	-170.73821	0.1 ± 0	5.8 ± 0.9	40.1 ± 6.8	0.007 ± 0.015	0.11 ± 0.24	1.5 ± 0.1	536.1 ± 76	47.2 ± 3.4	1.4 ± 0.3	19.3 ± 13.1	6.0 ± 0.3
Malaeloa-168	Well	1	-14.33358	-170.77082	0.1	7.0	23.8	0.008	0.00	5.8	675.8	31.5	5.6	7.5	6
Malaeloa-169	Well	2	-14.33337	-170.77319	0.1 ± 0	7.2 ± 0.1	28.1 ± 1.1	0.00 ± 0.00	0.63 ± 0.81	1.3 ± 0.4	655.3 ± 56.1	29.3 ± 1.4	1.2 ± 0.4	10 ± 7.1	5.9 ± 0.3
Pavaii-171	Well	3	-14.33373	-170.74288	0.8 ± 0.1	7.3 ± 0.1	84.2 ± 6	0.00 ± 0.00	0.59 ± 0.96	3.2 ± 0.2	778.2 ± 90.4	83.8 ± 3.3	3.1 ± 0.2	16.4 ± 7.2	9.0 ± 0.4
Pavaii-172	Well	1	-14.33531	-170.74393	1.1	6.9	79.7	0.000	0.00	2.8	769.4	81.3	2.6	15.8	8.5
Pavaii-177	Well	1	-14.33637	-170.75013	0.4	7.1	69.0	0.003	0.00	3.1	963.5	79.4	2.8	10.0	8.4
Pavaii-178	Well	1	-14.33650	-170.75485	0.1	7.4	33.7	0.000	0.10	1.0	780.9	39.2	1.0	20.0	7.7
Tafuna-33	Well	10	-14.32436	-170.73219	0.7 ± 0.4	6.0 ± 1.0	72 ± 13.3	0.003 ± 0.005	0.09 ± 0.12	1.5 ± 0.2	534.5 ± 59	80.2 ± 12.3	1.4 ± 0.3	19.4 ± 7.6	7.6 ± 0.3
Tafuna-61	Well	1	-14.32686	-170.73554	0.7	5.7	81.5	0.001	0.00	2.3	698.2	99.9	1.9	15.0	7.2
Tafuna-72	Well	1	-14.32154	-170.73219	0.2	6.1	62.3	0.001	0.00	1.9	499.9	70.2	1.8	12.5	7.5
Tafuna-77	Well	1	-14.32273	-170.73214	0.9	4.5	47.0	0.004	0.00	2.1	602.1	53.5	1.9	9.2	7.1
Tafuna-81	Well	1	-14.32065	-170.73203	0.1	5.2	46.2	0.000	0.10	2.5	469.2	46.2	2.7	32.5	6.9

Table C2. continued

Name	Type	n	Latitude	Longitude	Salinity [a.]	DO [a.] (mg/L)	NO_3^- [b.] (µM)	NO_2^- [c.] (µM)	NH_4^+ [d.] (µM)	PO_4^{3-} [e.] (µM)	SiO_4^{4-} [f.] (µM)	TN [g.] (µM)	TP [h.] (µM)	TOC [i.] (µM)	$\delta^{15}N_{(NO3-)}$ [j.] (‰)
CSp - 1	C. spring	2	-14.31969	-170.71535	3.4 ± 0.0	4.5 ± 0.4	42.2 ± 6.2	0 ± 0	0.09 ± 0.14	2.0 ± 0.3	449.6 ± 23.6	81.7 ± 6.9	1.9 ± 0.4	35.7 ± 19.2	9.1 ± 0.2
CSp - 2	C. spring	2	-14.34026	-170.78564	2.6 ± 0.0	7.0 ± 1.9	94.5 ± 5.9	0 ± 0	0.06 ± 0.09	3.7 ± 0.3	600.2 ± 24.4	92.6 ± 9.0	3.6 ± 0.1	35.6 ± 0.4	10.0 ± 1.2
CSp - 3	C. spring	1	-14.36480	-170.75971	0.3	2.9	1.7	0.000	0.00	2.4	708.6	4.3	2.2	77.5	6.7
CSp - 4	C. spring	1	-14.36067	-170.77632	0.5	5.0	4.7	0.162	0.00	3.8	1107.5	21.6	4.1	383.3	4.4
CSp - 5	C. spring	1	-14.35852	-170.75219	21.2	6.6	49.1	0.000	0.00	3.2	434.3	53.0	2.7	93.3	2.8
USp - 1	Up. spring	1	-14.31782	-170.74469	0.1	7.4	3.1	0.000	0.10	4.1	304.6	4.3	4.3	35.0	3.4
USp - 2	Up. spring	1	-14.33632	-170.75709	0.1	7.3	9.8	0.046	0.50	2.5	457.4	15.7	2.2	25.8	3.3
USp - 3	Up. spring	1	-14.31546	-170.79753	0.0	6.7	--	0.003	0.00	1.1	324.9	1.2	1.4	10.8	--

**Uncertainties shown with ± symbol indicate the standard deviation from averaged sample values. Uncertainties for data without a symbol are below.*

***a.** YSI factory reported instrument uncertainties: ±0.1 for salinity, ±0.1 mg/L for DO*

***b.** Nitrate uncertainty: ±1.2 µM*

***c.** Nitrite uncertainty: ±0.01 µM*

***d.** Ammonium uncertainty: ± 0.1 µM*

***e.** Phosphate uncertainty: ± 0.11 µM*

***f.** Silica uncertainty: ± 12.7 µM*

***g.** Total N uncertainty: ±3.2 µM*

***h.** Total P uncertainty: ± 0.2 µM*

***i.** Total organic C uncertainty: ± 0.29 µM*

***j.** $\delta^{15}N$ uncertainty: ±0.33‰*

REFERENCES

Almasri, M. N., & Kaluarachchi, J. J. (2007). Modeling nitrate contamination of groundwater in agricultural watersheds. *Journal of Hydrology*, *343*(3), 211-229.

Anderson, M.P., Woessner, W.W. (1992). *Applied groundwater modeling: simulation of flow and advective transport*. San Diego, CA: Academic Press.

Armstrong, F. A. J., Stearns, C. R., & Strickland, J. D. H. (1967). The measurement of upwelling and subsequent biological process by means of the Technicon Autoanalyzer® and associated equipment. *Deep Sea Research and Oceanographic Abstracts. 14*(3), 381-389.

AS-DOC - American Samoa Department of Commerce. (2013). *2013 Statistical yearbook for American Samoa*. (AS-DOC report). Pago Pago, American Samoa.

AS-EPA - American Samoa Environmental Protection Agency. (2005). *American Samoa Watershed Management and Protection Program Annual Report*. (AS-EPA report). Pago Pago, American Samoa.

AS-EPA - American Samoa Environmental Protection Agency. (2010). *Territory of American Samoa integrated water quality monitoring and assessment report* (AS-EPA 305[b] report). Pago Pago, American Samoa.

AS-EPA - American Samoa Environmental Protection Agency. (2013). *American Samoa Watershed Management and Protection Program Annual Report*. (AS-EPA report). Pago Pago, American Samoa.

AS-EPA - American Samoa Environmental Protection Agency. (2015). *GIS based piggery data for Tutuila and Manua islands.* [Data file].

AS-IPMC - American Samoa Interagency Piggery Management Council. (2004). *American Samoa water quality projects*. Retrieved from http://www.ctahr.hawaii.edu/rwq/american_samoa/projectsasipmc.htm

ASPA – American Samoa Power Authority. (2012). *Groundwater under the direct influence of surface water: Well 70.* (ASPA report). Pago Pago, American Samoa: Stephen Void, Josephine Regis, Karl Banks and Jason Gambatese.

Bishop, J. M., Glenn, C. R., Amato, D. W., & Dulai, H. (2015). Effect of land use and groundwater flow path on submarine groundwater discharge nutrient flux. *Journal of Hydrology: Regional Studies.* In Press, Available online 14 November, 2015

Bohl, H. P., Rothh, C., Tetzlaff, D., & Timmer, I. (2001). Estimation of groundwater recharge and nitrogen. *Proc. Aust. Soc. Sugar Cane Technol* (23), 84-89.

Böhlke, J.-K., (2003). *Sources, transport, and reaction of nitrate.* in: Lindsey, B.D., Phillips, S.W., Donnelly, C.A., Speiran, G.K., Plummer, L.N., Böhlke, J.-K.,Focazio, M.J., Burton, W.C., Busenberg, E., (Eds.) *Residence times and nitrate transport in ground water discharging to streams in the Chesapeake Bay Watershed*: (U.S. Geological Survey Water-Resources Investigations Report 03-4035). 25–39. http://pa.water.usgs.gov/reports/wrir03-4035.pdf.

Bouwman, A. F., Boumans, L. J. M., & Batjes, N. H. (2002). Estimation of global NH_3 volatilization loss from synthetic fertilizers and animal manure applied to arable lands and grasslands. *Global Biogeochemical Cycles, 16*(2).

Burkholder, J., Libra, B., Weyer, P., Heathcote, S., Kolpin, D., Thome, P. S., & Wichman, M. (2007). Impacts of waste from concentrated animal feeding operations on water quality. *Environmental health perspectives, 115*(2), 308-312.

CHEC - Charlotte Harbor Environmental Center. (2003). *Assessing the densities and potential water quality impacts of septic tank systems in the Peace and Myakka River Basins.* (CHEC report) Punta Gorda, FL. Retrieved from http://www.sarasota.wateratlas.usf.edu/upload/documents/Assessing_the_Density_Septics_Myakka.pdf

Chen B. (2013, April 15). ASPA water will be safe for consumption… but it will take time. *Samoa News.* Retrieved from http://www.samoanews.com/node/73942ASPA

Choudhary, M., Bailey, L. D., & Grant, C. A. (1996). Review of the use of swine manure in crop production: effects on yield and composition and on soil and water quality. *Waste Management & Research, 14(*6), 581-595.

Cole, M.L., K.D. Kroeger, J.W. McClelland, & I. Valiela. (2006). Effects of watershed land use on nitrogen concentrations and δ^{15}N nitrogen in groundwater. *Biogeochemistry 77*: 199-215.

Conan, C., Bouraoui, F., Turpin, N., de Marsily, G., & Bidoglio, G. (2003). Modeling flow and nitrate fate at catchment scale in Brittany (France). *Journal of Environmental Quality, 32*(6)*,* 2026-2032.

Coulter, J. W. (1941). Land Utilization in American Samoa. *Education*, *40*, 42 p.

Craig, P., (2002), Natural history guide to American Samoa; a collection of articles, in Craig, P., ed., National Park Service and the Department of Marine and Wildlife Resources.

Dailer, M. L., Smith, J. E., & Smith, C. M. (2012). Responses of bloom forming and non-bloom forming macroalgae to nutrient enrichment in Hawai‘i, USA. *Harmful Algae, 17*, 111-125.

DiDonato, G. T. (2005). Nitrogen and phosphorus concentrations in tropical Pacific insular streams: historical data from Tutuila, American Samoa. *Micronesica-Agana-, 37*(2), 235.

DiDonato, G. T., & Paselio, E. B. (2006). Localized beach contamination in American Samoa: Results from two years of weekly monitoring. *Marine pollution bulletin*, 52(4), 466-468.

El-Kadi A.I., Yabusaki K. (1996*). Assessment of nutrient use and nitrate contamination in central Oahu, Hawaii.* (Water Resources Research Center, University of Hawaii at Manoa report*,* 1996-07). Honolulu, HI.

Eyre, P. (1994). *Ground-water quality reconnaissance, Tutuila, American Samoa, 1989*. (US Department of the Interior, US Geological Survey. Water-Resources Investigations Report 94-4142). Honolulu, HI.

Falkland, T. (2002). Proceedings from: Pacific Regional Consultation on Water in Small Island Countries, 29 July–3 August 2002. *Towards sustainable water management in the Pacific*. Sigatoka, Fiji.

Fenech, C., Rock, L., Nolan, K., Tobin, J., & Morrissey, A. (2012). The potential for a suite of isotope and chemical markers to differentiate sources of nitrate contamination: a review. *Water research, 46*(7), 2023-2041.

Gardner, K. K., & Vogel, R. M. (2005). Predicting ground water nitrate concentration from land use. *Ground water, 43*(3), 343-352.

Gelhar, L.W., Welty, C., & Rehfeldt, K. (1992). A critical review of data on field- scale dispersion in aquifers. *Water Resources Research 28* (7), 1955–1974.

Glenn, C. R., Whittier, R. B., Dailer, M. L., Dulaiova, H., El-Kadi, A. I., Fackrell, J., ... & Sevadjian, J. (2013). *Lahaina groundwater tracer study—Lahaina, Maui, Hawai ʻi, Final Report.* (Prepared for the State of Hawai ʻi Department of Health, the US Environmental Protection Agency, and the US Army Engineer Research and Development Center). Honolulu, HI

Grasshoff, K., Kremling, K., & Ehrhardt, M. (Eds.). (1983). *Methods of seawater analysis*. Weinheim (Federal Republic of Germany) John Wiley & Sons.

Harbaugh, A. W. (2005). *MODFLOW-2005, the US Geological Survey modular ground-water model: the ground-water flow process.* (US Department of the Interior, US Geological Survey report). Reston, VA.

Hinkle, S. R., Böhlke, J. K., & Fisher, L. H. (2008). Mass balance and isotope effects during nitrogen transport through septic tank systems with packed-bed (sand) filters. *Science of the total environment, 407*(1), 324-332.

Hrudey, S. E., & Hrudey, E. J. (2007). Published case studies of waterborne disease outbreaks—evidence of a recurrent threat. *Water Environment Research*, *79,* 233-245.

Hunt, C. D. (2007). *Ground-water nutrient flux to coastal waters and numerical simulation of wastewater injection at Kihei, Maui, Hawaii* (US Department of the Interior, US Geological Survey report No. 2006-5283). Honolulu, HI.

Hunt Jr, C. D., & Rosa, S. N. (2009). *A multitracer approach to detecting wastewater plumes from municipal injection wells in nearshore marine waters at Kihei and Lahaina, Maui, Hawaii* (US Department of the Interior, US Geological Survey report No. 2009-5253). Honolulu, HI.

Izuka, S. K., Perreault, J. A., & Presley, T. K. (2007). *Areas Contributing Recharge to Wells in the Tafuna-Leone Plain, Tutuila, American Samoa* (US Department of the Interior, US Geological Survey report No. 2007-5167). Honolulu, HI.

Izuka, S. K. (2011). *Potential effects of roadside dry wells on groundwater quality on the Island of Hawai'i-Assessment using numerical groundwater models.* (US Department of the Interior, US Geological Survey report). Honolulu, HI.

Kantor, M., Baker, D.J., Wilson, W.S. (1996). *Territory of American Samoa Coastal Non-Point Pollution Control Program.* (National Oceanic and Atmospheric Administration Report). Silver Spring, MD. Retrieved from: http://www.reefbase.org/pacific/pub_E0000006414.aspx

Kendall, C. and McDonnell, J. J. (1998). *Isotope Tracers in Catchment Hydrology* (Eds.). Elsevier Science B.V., Amsterdam. pp. 519-576.

Kendall, C., and R. Aravena. (2000). Nitrate isotopes in groundwater systems. In: *Environmental Tracers in Subsurface Hydrology*, Eds. P. Cook, and A.L. Herzerg, pp. 261-297, Klewar Academic, Boston.

Kennedy/Jenks/Chilton. (1987). *Groundwater Contamination Study: Tafuna-Leone Plain, Tutulla Island.* (Report submitted to the Environmental Quality Commission Office of the Governor Tutulla, American Samoa). Honolulu, HI.

Knight Enterprises Inc. (2014). *Assessment for Alternative Water Resources on Tutuila, American Samoa*. (Report submitted to American Samoa Power Authority). Honolulu, HI: Michael D. Knight

Krause, P., Boyle, D. P., & Bäse, F. (2005). Comparison of different efficiency criteria for hydrological model assessment. *Advances in Geosciences, 5,* 89-97.

Lee, C., Hristov, A. N., Cassidy, T., & Heyler, K. (2011). Nitrogen isotope fractionation and origin of ammonia nitrogen volatilized from cattle manure in simulated storage. *Atmosphere, 2*(3), 256-270.

Legates, D. R., & McCabe, G. J. (1999). Evaluating the use of "goodness-of-fit" measures in hydrologic and hydroclimatic model validation. *Water resources research*, *35*(1), 233-241.

Ling, G., & El-Kadi, A. I. (1998). A lumped parameter model for nitrogen transformation in the unsaturated zone. *Water Resources Research, 34*(2), 203-212.

Liu, Z., Gurr, N. E., Schmaedick, M. A., Whistler, W. A., & Fischer, L (2011). Vegetation Mapping of American Samoa. (General Technical Report. US Department of Agriculture, Forest Service, Pacific Southwest Region). Vallejo, CA

Mair, A., & El-Kadi, A. I. (2013). Logistic regression modeling to assess groundwater vulnerability to contamination in Hawaii, USA. *Journal of contaminant hydrology*, *153*, 1-23.

McCuen, R.H., & Snyder, W.M., (1986). *Hydrologic Modeling: Statistical Methods and Applications.* Englewood Cliffs, NJ: Prentice Hall.

McDougall, I. (1985). Age and evolution of the volcanoes of Tutuila, American Samoa, *Pacific Sci*., *39*, 311–320.

Miller, M. (2013,October 22) American Samoa authorities investigate pesticide use by foreign farmers. *Radio New Zealand International Podcast*. Podcast retrieved from: http://www.radionz.co.nz/international/programmes/datelinepacific/audio/2573683/american-samoa-authorities-investigate-pesticide-use

Morgan, D. S., Hinkle, S. R., & Weick, R. J. (2007). Evaluation of approaches for managing nitrate loading from on-site wastewater systems near La Pine, Oregon. (US Department of the Interior, US Geological Survey report 2007-5237) Reston, VA.

NRCS. (2007). *Issue Paper, Piggery Waste Management in American Samoa*. (United States Department of Agriculture report). Honolulu, HI.

Oki, D. S., & Giambelluca, T. W. (1987). DBCP, EDB, and TCP contamination of ground water in Hawaii. *Ground Water, 25*(6), 693-702.

Perry, J. (1986). *American Samoa resource assessment: a statement of conditions for long-range planning*. (American Samoa Community College Land Grant Program technical report). Pago Pago, American Samoa

Ransom, K. (2015, December). *Bayesian nitrate source apportionment to individual groundwater wells in the Central Valley by use of elemental and isotopic tracers*. Poster session presented at the American Geophysical Union Annual Meeting, San Francisco, CA.

Savoie, D. L., Prospero, J. M., & Nees, R. T. (1987). Washout ratios of nitrate, non-sea-salt sulfate and sea-salt on Virginia Key, Florida and on American Samoa. *Atmospheric Environment, 21*(1), 103-112.

Schulze-Makuch, D. (2005). Longitudinal dispersivity data and implications for scaling behavior. *Ground Water*, 43(3), 443-456.

Siegrist, R. L., Tyler, E. J., & Jenssen, P. D. (2000). *Design and performance of onsite wastewater soil absorption systems.* (White paper prepared for National Needs Conference, Risk-Based Decision Making for Onsite Wastewater Treatment). St. Louis, MO pp. 19-20.

Sigman D.M., K.L. Casciotti, M. Andreani, C. Barford, M. Galanter and J.K. Bohulke. (2001). A bacterial method for the nitrogen isotopic analysis of nitrate in seawater and freshwater. *Analytical Chemistry, 73,* 4145-4153.

Stearns, H. T. (1944). Geology of the Samoan islands. *Geological Society of America Bulletin*, *55*(11), 1279-1332.

Thornthwaite, C.W. and Mather, J.R. (1955). The water balance. *Publications in Climatology, 8*, 1-104.

Todd, D. K., & Mays, L. W. (1980). Groundwater hydrology. New York, NY: John Wiley and Sons.

US-DOA - Department of Agriculture (2011). *American Samoa 2003 Census of Agriculture. Vol. 1, Part 55.* (United States Department of Agriculture report) Retrieved from: http://www.agcensus.usda.gov/Publications/2002/Dates_for_Ag_Census_Reports/

Valiela, I., Collins, G., Kremer, J., Lajtha, K., Geist, M., Seely, B., ... & Sham, C. H. (1997). Nitrogen loading from coastal watersheds to receiving estuaries: new method and application. *Ecological Applications, 7*(2), 358-380.

Van Cuyk, S., Siegrist, R., Logan, A., Masson, S., Fischer, E., & Figueroa, L. (2001). Hydraulic and purification behaviors and their interactions during wastewater treatment in soil infiltration systems. *Water Research, 35*(4), 953-964.

Verstraeten, I. M., Fetterman, G. S., Meyer, M. T., Bullen, T., & Sebree, S. K. (2005). Use of tracers and isotopes to evaluate vulnerability of water in domestic wells to septic waste. *Groundwater Monitoring & Remediation, 25*(2), 107-117.

Viers, J. H., Liptzin, D., Rosenstock, T. S., Jensen, W. B., & Hollander, A. D. (2012). *Nitrogen sources and loading to groundwater.* In Technical Report 2, Assessing Nitrate in California's Drinking Water Center for Watershed Sciences, University of California Davis, CA. p. 326.

Walker, G. P., & Eyre, P. R. (1995). Dike complexes in American Samoa. *Journal of volcanology and geothermal research, 69*(3), 241-254.

Whittier, R. B., & El-Kadi, A. (2009*). Human and Environmental Risk Ranking of Onsite Sewage Disposal Systems.* (State of Hawaii, Department of Health Safe Drinking Water Branch report). Honolulu, HI.

The World Bank. (2015). *Fertilizer consumption (kilograms per hectare of arable land).* [Data file]. Retrieved from http://data.worldbank.org/indicator/AG.CON.FERT.ZS?page=2

WSDH - Washington State Department of Health (2002). *Rule Development Committee Issue Research Report Draft – Residential Flow Rates*. (Washington State Department of Health report). Tumwater, WA: Benefield, L. A.

Xu, M., Eckstein, Y., 1995. Use of weighted least-squares method in evaluation of the relationship between dispersivity and field scale. *Ground Water, 33*(6), 905–908.

Zennaro, B. (2007, Fall). Regulating illegal piggery waste runoff. *ArcNews Online.* Retrieved from http://www.esri.com/news/arcnews/fall07articles/regulating-illegal.html

Zheng, C. and P.P. Wang, (1999). *MT3DMS: A modular three-dimensional multispecies model for simulation of advection, dispersion and chemical reactions of contaminants in groundwater systems; Documentation and User's Guide.* (U.S. Army Engineer Research and Development Center Contract Report SERDP-99-1). Vicksburg, MS.